Investigation of Thermoluminescence Properties of Calcite ($CaCO_3$)

M.Sc.Thesis

in

Engineering Physics

University of Gaziantep

Supervisor

Assist. Prof. Dr. R.Güler Yıldırım

BY

Esen Gün

2006

Approval of the Graduate School of Natural and Applied Sciences

_____

Prof. Dr. Sadettin ÖZYAZICI
Director

I certify that this thesis satisfies all the requirements as a thesis for the degree of Master of Sciences.

_____

Prof. Dr. Zihni ÖZTÜRK
Head of Department

This is to certify that we have read this thesis and that in our opinion it is fully adequate, in scope and quality, as a thesis for the degree of Master of Science.

_____

Assist. Prof. Dr. R.Güler YILDIRIM
Supervisor

Examining Committee Members

Prof. Dr. Zihni ÖZTÜRK _____

Prof. Dr. Melda Ö. ÇARPINLIOĞLU _____

Assoc. Prof. Dr. A.Necmettin YAZICI _____

Assist. Prof. Dr. R.Güler YILDIRIM _____

Assist. Prof. Dr. Mustafa ÖZTAŞ _____

ABSTRACT

Investigation of Thermoluminescence Properties of Calcite ($CaCO_3$)

GÜN Esen

M.Sc., in Physics Engineering

Supervisor: Assist. Prof. Dr. R.Güler YILDIRIM

February 2006, 65 pages

The thermoluminescence characteristics of calcite samples of annealed and unannealed has been studied that were beta irradiated at different dose levels in this study. The additive dose (AD), variable heating rate (VHR), initial rise (IR), computer glow curves deconvolution (CGCD) and peak shape (PS) methods have been used for the evolution of TL glow peaks. These methods were used to determine the number of peaks and kinetic parameters (activation energy E, attempt-to-escape frequency factor s and kinetic orders b). The calcite samples that were collected from Gaziantep city exhibit two main TL peaks following β irradiation between the dose levels 0.9 Gy and 864 Gy. The results indicate that kinetic parameters that obtained vary fairly from the different methods. The glow curves of annealed and unannealed sample irradiated with beta dose show main peaks at (115 and 254 ^{0}C). The enhancement in TL sensitivity was found to be depending on the annealing temperature and time. The measurement of the dose responses and fading

process are very useful in radiation dosimetry and archeological dating. The dose response of all peaks have shown a similar pattern. First they follow strong linearity and then saturate at different dose levels. After the storage at room temperature for four weeks, peak 1 was completely disappeared from the glow curves, but peak 2 was not affected during this period. Peak 1 is reduced to typically 36% of its original value at the end of 2 hours and 70% its original value at the end of 6.5 hours. The glow curve structure of calcite was also studied by additive dose method in this study and it was observed that its glow curve is the superposition of at least two first order glow peaks.

Keywords: thermoluminescence, annealing, unannealing, kinetic parameters, calcite.

ÖZET

Kalsit'in ($CaCO_3$) Termoluminesans Özelliklerinin Araştırılması

GÜN Esen
Yüksek Lisans Tezi
Gaziantep Üniversitesi, Fizik Mühendisliği Bölümü
Tez Danışmanı: Yrd. Doç. Dr. R.Güler YILDIRIM
Şubat 2006, 65 sayfa

Bu çalışmada, kalsit maddesinin termoluminesans karakteristiği farklı oranlardaki beta dozlanmasıyla tavlı ve tavsız çalışılmıştır. Termal ışıldama tepeciklerini değerlendirmek için Doz Ekleme (AD), ilk yükselme (IR), değişken ısıtma sıcaklığı oranı (VHR), bilgisayar ile ışıldama eğrisi ayrışımı (CGCD) ve ışıldama eğrileri şekli (PS) kullanıldı. Bu metodlar termal ışıldama eğrileri ve bu eğrileri oluşturan ışıldama tepeciklerinin kinetik parametrelerini (aktivasyon enerjisi E, frekans faktörü s and kinetik derecesi b) incelemek için kullanılmıştır. Gaziantep şehrinden alınan kalsit örneği 0.9 Gy ile 864 Gy arasında beta ışını ile ışıldandığında iki belirgin termal ışıldama tepesi göstermiştir. Kinetik parametre sonuçları uygulanan metodlara göre değişiklikler göstermiştir. Beta radyasyonu ile dozlanan tavlı ve tavsız kalsit örneği 115 ve 254 ^{0}C de iki belirgin ışıldama eğrisi tepeciği göstermiştir. Termoluminesans duyarlılığındaki artış tavlama sıcaklığı ve zamanına bağlı olduğu görülmüştür. Radyasyon dozimetresinde ve arkeolojik yaş tayinlerinde

oldukça kullanışlı olan doz tepkisi eğrisi ve zaman ile sönüm işlemi kullanılan materyal için incelenmiştir. Bütün tepeciklerin doz tepkisi aynı modeldedir, öncelikle uygulanan doz miktarı ile çizgisel olarak artar ve ardından farklı dozlarda doyuma ulaşırlar. Karanlık bir ortamda dört hafta bekletildikten sonra birinci ışıldama tepeciği tamamen kaybolmuş fakat ikinci ışıldama tepeciği değişmemiştir. İki saat sonunda birinci ışıldama tepeciği orijinal değerinden % 36 azalmıştır ve altı buçuk saat sonunda ışıldama tepeciği orijinal değerinden % 70 azalmıştır. Ayrıca doz ekleme metodu kullanarak kalsitin ışıldama eğrileri detaylıca çalışılmış ve bu materyalin ışıma eğrilerinin iç içe geçmiş birinci dereceden iki tane ışıldama tepeciğinden oluştuğu görülmüştür.

Anahtar kelimeler: termoluminesans, tavlı, tavsız, kinetik parametreler, kalsit

ACNOWLEDGEMENT

I would like to thank my supervisor Assist. Prof. Dr. R.Güler YILDIRIM for her guidance, suggestion, advice, and help in the preparation of this study. I am deeply indepted to her for all efforts and helping me to overcome all the barriers I encountered throughout this study.

I wish to thank Assoc. Prof. Dr. A.Necmettin YAZICI for providing me materials on thermoluminescence, his advices and helps during this work.

I wish to thank Research Assistant Vural Emir KAFADAR for assisting me in carrying out experiments and obtaining experimental result.

I also want to thank the my mother for supporting and encouraging me.

CONTENTS

LIST OF TABLE page

LIST OF FIGURES

CHAPTER 1

INTRODUCTION

Thermoluminescence (TL) is a result of high energy electrons trapped within the specimen after the irradiation by radiation. Thermoluminescence phenomena can be observed at semiconductor and insulator which contain electrons trapped at defect sites in a metastable condition. The trapped charge can be liberated by heat and will cross the potential barrier and move to a lower energy state with the emission of light. This is called thermoluminescence [1].

Thermoluminescence is observed under condition of steadily increasing temperature. In the usual thermoluminescence experiments, the TL system is irradiated at room temperature (RT) and later heated through a temperature range where the luminescence is bright, until a temperature level at which all the charges have been thermally excited out of their metastable levels and the luminescence completely disappears. If the light intensity is plotted as a function of temperature (or time) the resulting graphs is called glow-curve [2].

Thermoluminescence (TL) method is a relatively complex process since it involves a trap and a luminescence centre. When an insulator or semiconductor is exposed to ionizing radiation at room or low temperature, electrons are released from the valance band (VB) to the conduction band (CB). This leaves a hole in the valance band. Both types of carriers become mobile in their respective bands until they recombine or until they are trapped in lattice imperfections in the crystalline solids. These lattice imperfections play very crucial role in the TL process. The trapped electrons may remain for a long period when the crystals are stored at room temperature or they can be released due to the sufficient energy given to the electrons when the crystal is heated. These electrons may move in the crystalline solid until they recombine with suitable recombination centres that contain hole with the emission of TL light. This process of light emission by thermal stimulation from a

crystalline solid after irradiations is called as “thermally stimulated process” or simply thermoluminescence”.

In thermoluminescence phenomena can be found the tree essential ingredients necessary for the productions of thermoluminescence. Firstly, the material must be an insulator or a semiconductor-metal do not exhibit luminescent properties. Secondly, the material must have at some time absorbed energy during exposure to radiation. Thirdly, the luminescence emission is triggered by heating the material. In addition, there is one important property of thermoluminescence which cannot be inferred from this statement as it stands at present. It is a particular characteristic of thermoluminescence that, once heated to excite the light emission, the material cannot be made to emit thermoluminescence again by simply cooling the specimen and reheating. In order to re-exhibit luminescence the material has to be re-exposed to radiation, whereupon raising the temperature will once again produce light emission. The fundamental principles which govern the production of thermoluminescence are essentially the same as those which govern all luminescence process, and in this way thermoluminescence is merely one of a large family of luminescence phenomena [3].

Efficient thermoluminescent phosphors have a high concentration of electron and hole traps, provided by structured defects and impurities [2]. The calcite sample can be contained with Mn^{+2}, Pb^{+2} or Fe^{+3} e.g., either individually or simultaneously with more than one of these in impurities. Transition is the excitation of a valance electron from a host atom into the conduction band in which state it has enough energy to move freely through the lattice. Transitions correspond to the process of ionization and are a result of the absorption of energy from external sources, e.g. radiation. During absorption of light in the far ultraviolet or irradiations with alpha, beta and gamma corresponds to the liberation of an electron from the valance band into conduction band (leaving a hole in the valance band) [4].

Thermoluminescence properties of crystal calcite commonly were studied. Calcite is one of the most common and widespread minerals found in the limestone deposit which is a very common sedimentary rock [5]. Structure of calcite is hexagonal. The calcite structure is described as a NaCl type arrangement of (Ca) cations and (CO_3) anionic groups [6]. Examples of insulators are cubic structure alkali halides, such LiF and NaCl. The thermoluminescence (TL) of calcite ($CaCO_3$ crystal of trigonal symmetry) has been studied by several workers [7].

Many natural crystals exhibit thermoluminescence (TL) properties that are suitable for TL dating. Thermoluminescence (TL) has become an important tool for the dating of archaeological and geological materials [3]. Furthermore; materials of interest in thermoluminescent dosimetry (TLD) which are principally insulators which electrons are entirely due to absorbed radiation energy. Consequently; investigations on calcite have shown different TL characteristics depending on the impurity content and on the genesis of the sample. It was also observed on artificially grown $CaCO_3$ crystals that the type and concentration of impurities modify both TL sensitivity and glow-curve shape. Many natural crystals exhibit TL properties that are suitable for TL dating. The determination of the kinetic parameters is therefore an active area of research and various techniques have been developed to derive the parameters from the glow curve. David and colleagues recorded the glow curves from several different natural specimens and emphasized that it is difficult to compare the published TL from different specimens because of differences in heating rates, pre-irradiation treatment, impurity content, method of manufacture etc. [8].

The aim of this study is to determine the kinetic parameters, dose response and stability of TL peak of natural calcite. There are various methods for evaluating the kinetic parameters from TL glow curves [4]. When one of glow peaks is highly isolated from others, the experimental methods such as initial rise (IR), variable heating rates (VHR), computer glow curves deconvolution (CGCD) and peak shape (PS) methods are suitable methods to determine these parameters. However as in most TL materials, the glow curve of calcite consist of several overlapping peaks. When more than one glow peak is present in the glow curve, there are essentially two ways to obtain these parameters: the first way is to isolate each individual TL peak from others using partial thermal annealing treatment and the second way is to make a complete glow curve analysis using deconvolution [9].The difficulty arises in the first method due to the problems in isolating the peak of interest without any loss of intensity. The major attractive feature of the deconvolution technique is the simultaneous determination of kinetic parameters of all peaks with no treatment. However, deconvolution method has also its disadvantages over the classical methods in some cases; especially the structure of glow curve is very complex. Therefore, different methods together with deconvolution method have been used to determine the kinetics parameters of calcite due to some difficulties in interpreting the deconvolution. These methods are AD, IR, VHR, CGCD and PS. We obtain two

main glow curves at 115 and 253 ^{0}C from calcite samples, which have been collected from Gaziantep city, following beta irradiations. Glow curves from calcite sample following different doses show that TL peaks occur more or less at the same temperature, whereas the intensities of the peaks change relative to each other.

CHAPTER 2

LITERATURE SURVEY

Dose rate effect in calcite was examined by M.Urbina, A.Millan, P.Benitz and T.Calderon [5].This study of the evolution of thermoluminescence versus gamma and beta irradiation with a different dose rate, has been made for calcite samples previously γ-irradiated at a fixed dose rate for a long time are later γ-irradiated, the relative populations of created centers seems to be characteristic of the last irradiation. The reverse effect has also been observed. In fact that research describes a dose rate effect in terms of dynamic equilibrium during irradiation between F and M centers. A second important consequence of this dose rate effect could be the possibility to calculate the previous gamma dose applied to calcite samples if these are optically bleached by sunlight exposure.

S.Drendrajit Singh and Ingotombi examined thermoluminescence glow curve of γ-irradiated calcite [6]. Both colourless and brown varieties of calcite found in the sedimentary lime stone deposits of Ukhrul, Manipur (India) have been used in that study. The natural TL of these samples is weak. Hence, glow curves of γ-irradiated materials have been used for analysis. The presence of five TL peaks in calcite was well established. The trapping parameters, namely the activation energy E, frequency factor s and b order of kinetics of the thermoluminescence (TL) peaks of calcites (brown and colourless varieties) irradiated with 4.08 kGy of γ rays, are determined using the least-squares curve-fitting technique. The electron lifetime τ of the peaks of calcite is calculated in order to estimate the upper limit of their utility in TL dating. Both the brown and colourless varieties of calcite generated in limestone deposits of sedimentary rocks do not show any prominent TL peak near 280 ^{0}C in agreement with the earlier finding, although for brown calcite the presence of this peak could be revealed while fitting the total glow curve. The absence of 280 ^{0}C may be due to the total glow curve. The order of kinetic of the TL peaks of calcite is found to be 2 except for the 180 ^{0}C peak. The lifetimes of the 230 ^{0}C and 330 ^{0}C peaks are 1330

years and $1.8x10^8$ years, respectively. The colourless calcite has a peculiar characteristic behaviour different from that of brown calcite showing a prominently strong TL peak at around 330-340 ^{0}C comparable with the 220-245 ^{0}C peak.

Local transitions and charge transport in thermoluminescence of calcite was investigated by Y.Kirsh, PD. Townsendand S, Shoval at university of Sussex in U.K. [7]. Colourless, natural calcite single crystals exhibit several distinct TL peaks following x-irradiation at room temperature in this research. The purpose of that work was to evaluate the kinetic parameters of TL peaks by applying standard methods of analysis, namely the initial rise technique, and a best fit programme which seeks the parameters optimally describing the experimental TL curve. Kinetic analysis of the main peak at about 80 ^{0}C discloses a continuous spectrum of traps having the same activation energy, 0.73 eV and distribution of frequency factors. Four additional peaks at 152, 179, 254 and 296 ^{0}C were obtained having activation energies of 0.92, 1.01, 1.52 and 1.70 eV respectively. The kinetic data and the analysis of the emission spectra ascribes the 80 ^{0}C peak to local transitions such as tunnelling, and the higher temperature peaks to processes which involve transport of ionic charge-carries.

Vasilis Pagonish and Christodoulous Michaeli investigated annealing effects on the thermoluminescence of synthetic calcite powder [10]. They have studied the effect of annealing temperature on the nature and kinetics of the thermoluminescence (TL) trapping center of synthetic calcite. The energy values for the traps associated with the observed TL peaks were measured using the initial rise method and were used as input for a least-squares fit procedure, which expresses the TL glow curves as the sum of five individual peaks of general order kinetics. It was found that all experimental TL glow curves for different annealing temperatures and various doses could be fitted to the same set of kinetic parameters E, s and b indicating that the annealing process probably does not change the nature of the trapping centers. The activation energy for the change in sensitivity with annealing temperatures was found using Arrheius-type plots for each TL peak. Their research show that the change in sensitivity of synthetic calcite samples annealed in air can be attributed to changes occurring within the luminescence center and that no apparent changes take place in trapping center themselves.

Vasilis Pagonish, Eric Allman and Albert Wooten examined thermoluminescence from a distribution of trapping levels in UV irradiated calcite

[11]. Different calcite samples have been studied in this study. Both geological and synthetic calcite samples exhibit a low temperature thermoluminescence (TL) peak around 80 ^{0}C, this TL peak has been the subject of several investigations since it is believed to involve localized transitions in the crystal rather than the more usual electronic transitions through the energy bands. Their experimental results are consistent with the presence of distribution of activation energy and first order TL process associated with this TL peak. Various methods were used to evaluate the activation energy E, the frequency factor s and the order of the kinetics b. Good agreement was obtained between all methods expect the isothermal decay method. A theoretical model based on Gaussian distribution of energies provides a self consistent description of the TL glow curves and the dose dependence of the observed TL height. When the calcite sample is annealed at temperatures above 500 ^{0}C, the width of the Gaussian distribution of energies becomes narrower.

Birol Engin and Olgun Güven have made a research on "the effect of heat treatment on the thermoluminescence of naturally-occurring calcites and their use as a gamma ray dosimeter" [12]. Within the research; the feasibility of using naturally-occurring calcite for gamma-ray dosimetry was investigated. Ionizing radiation dosimeters, which rely on the thermoluminescence properties of materials, have helped in the solutions of many dosimetric problems due to their long time storage capacities, independence of dose with radiation intensities, ease with which measurements are done and light weights. Three calcites of very different origin were used in this study. The first calcite was satalactite (speoleothem) collected from the geologically important cave of Gökgöl (Zonguldak) in northern Turkey. The second geological calcite was a flowstone from the Damlataş cave in southern Turkey. The third type of geological calcite was marble from Marmara islands (Balıkesir) of Turkey. The thermoluminescence and dosimetric characteristics of the tree different original calcite materials were studied after different thermal treatments as well as applications for determination of low and intermediate gamma doses in that study. These were stored in the dark. For studying the effect of thermal treatment, the natural calcite samples were annealed in air atmosphere at temperatures ranging from 200 to 700 ^{0}C. Annealed samples were also irradiated with ^{60}Co gamma irradiation of different dose rates. Annealing produces changes in the sensitivity of all calcite samples to ionizing radiation. Annealing increases the intensity of all glow peaks expect the peaks above 300 ^{0}C. The dose response curves were also established for

the stable dosimetric peaks of unannealed calcite samples. These dose-response curves could also be fitted with the same linear mathematical function, but differed by proportionality factor. According to these findings, the dose-response of the trapping center of dosimetric peaks remains unaffected by annealing process. These results have also shown that the annealing procedure of the samples does not change the properties of the trapping centers.

Thermoluminescence mechanism of Mn^{+2}, Mg^{+2} and Sr^{+2} doped calcite was investigated by Z.S. Macedo, M.E.G. Valerio and J.F. De Lima [13]. In this work, the properties of synthetic crystal of doped calcite were studied. Samples were doped with Mn^{+2}, Mg^{+2} or Sr^{+2}, either individually or simultaneously with more than one of these impurities. TL glow-curves, partial heating measurement, isometric curves, emission spectra and thermal treatment were performed, in order to investigate the role played by the impurities in the TL glow peaks of calcite. They conclude that the crystals doped with Mn^{+2} show five TL peak with emission spectra due only to the Mn^{+2}. The relative intensity of these peaks is closely related to the other divalent dopant added in the solution (Sr^{+2} or Mg^{+2}). These results suggest that although Sr^{+2} and Mg^{+2} act as TL activators stabilising slightly different electron traps, they are not directly connected to the Mn^{+2} luminescence centre.

J.F.de Lima , M.E.G. Valeriao and E.Okuno investigated the effect of gamma and ultraviolet radiations on the thermoluminescence of Brazilian calcite [14]. The irradiated samples presented three thermoluminescence (TL) peaks at 150, 245 and 320 ^{0}C with a main emission band centered at 615 nm due to the ^4G-^6S transitions of the Mn^{+2} ESR signals, three lines related to carbonate groups. The thermal treatment and irradiations effects on the electron spin resonance signed lead to the conclusion that $(CO_3)^{-3}$, stabilized in two different symmetries, and the $(CO_2)^-$ ions are the electron trapping centres. It was found that the TL peaks follow a t^{-1} decay as a function of UV illumination time. An alternative model for the TL emission of calcite is discussed, considering that the recombination of charges is processed via thermally assisted tunnelling mechanism. Their results observed clearly establish the role of the $(CO_3)^{-3}$ and (CO^{-2}) ions as the main trapping centres and the role of Mn^{+2} as the recombination and the luminescence centre in the TL process in the calcite. The recombination of charges between the electron and the hole traps are via a tunnelling process. If that happens, both centers should be close enough to enable the tunnelling process to take place. Hence, they suggest that during the irradiation of the

samples the $(CO)^{3-}$ and $(CO)^{-2}$ centres are formed in the vicinity of a Mn^{+3} substituting for a Ca^{+2} of the calcite matrix.

V.Ponnusamy, V.Ramasam, M.Dheenathayalu and J.Hemalatha investigated "effect of annealing in thermostimulated luminescence (TSL) on natural blue colour calcite crystals" [15]. In this study, the thermostimulated luminescence (TSL) glow curve characteristics of 10 blue coloured calcite crystal of Southern Tamilnadu were analysed. The natural thermoluminescence measurements were carried out for all the samples and annealed in air at the temperatures ranging from 200 to 700 ^{0}C. The glow curves of annealed or unannealed samples irradiated with a gamma dose of 500 Gy show three peaks at 145, 225 and 345 ^{0}C. The enhancement in TSL sensitivity was found to depend on the annealing temperature and time. The response to gamma irradiation is linear in the range from 1 to 10^4 Gy. The emission spectra of all the samples show an emission at around 610 nm but with different intensities for each sample. With reference to earlier work, it may be assumed that the recombination site always involves Mn^{+2} ions.

CHAPTER 3

Theory of Thermoluminescence

3.1. Luminescence Phenomena

Luminescence is the emission of light from certain solid called phosphors. This emission, which does not include black body radiation, is the release of energy stored within the solid through certain types of prior excitation of the electronic system of solid. This ability to store is important in luminescence dosimetry and is generally associated with the presence of activators [16]. Luminescence, unlike natural radioactivity, does not occur spontaneously but, generally requires energy to excite it. The excitation can be caused by ultraviolet light, x-rays, gamma rays, electron or alpha particles, all of which can deposit energy into material that is subsequently reemitted in the from of visible light. Luminescence properties of various types of material can be obtained. [3]

The light emitted, when the electron comes back to its ground energy level, can be classified according to a characteristic time, τ, between the absorption of the exciting energy and emission of light. If this time is less than 10^{-8} sec, the luminescence is called fluorescence. The light is emitted with a wavelength larger than the wavelength of the absorbed light owing to dispersion of energy by the molecule. If the time between absorption and emission is larger than 10^{-4} sec, the luminescence is then called phosphorescence. The process of phosphorescence is explained with the presence of a metastable level, between the fundamental and the excited levels, which acts as a trap for the electron [17, 18, 19].

3.2. Crystal Structures and Crystal Defects

3.2.1 Alkali Halides and $CaCO_3$ (calcite)

The alkali halides are typical ionic compounds, and their physical properties are in general well known. The majority of the alkali halides crystallize in the rock salt structure, as shown in Figure 3.1. In this structure each cation (alkali metal ion M^+) is surrounded by six nearest-neighbour anions (halogen ions X^-) and each by six nearest - neighbour cations. The cations and anions are each situated on the points of separate face-centered cubic lattices, and these two lattices are inter-leaved with each other.

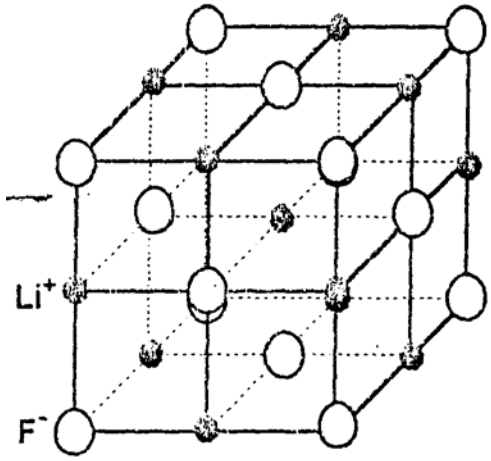

Figure 3.1 The structure of the rock salt (NaCl) type alkali halides.

Many chemical impurities, when incorporated in the alkali halides even in parts-per-million (ppm), affect the physical and chemical properties of alkali halides. When the temperature is raised, the electrical conductivity increases very rapidly. The carriers of electric charge are ionic in nature, not electronic. An insulator, like an alkali halide, can be described quantum mechanically by the band model. For a crystal without lattice defects there are no energy levels between the valance and conduction bands. The energy levels introduced may be discrete, or may be distributed depending upon the exact nature of the defect and of the host lattice. In general terms, it is believed that the lattice imperfections, impurities, intrinsic and extrinsic defect give rise to localized energy levels (metastable state) within the

forbidden energy gap and they may be well understood using the example of an alkali halide crystal of the type $M^{+}X^{-}$.

Calcite is one of the most common and widespread minerals found in limestone deposits which is described as a NaCl type, arrangement of ($Ca^{+2)}$ cations and (CO^{-2}) anionic groups. Calcite is trigonal symmetric. (Fig.3.2)

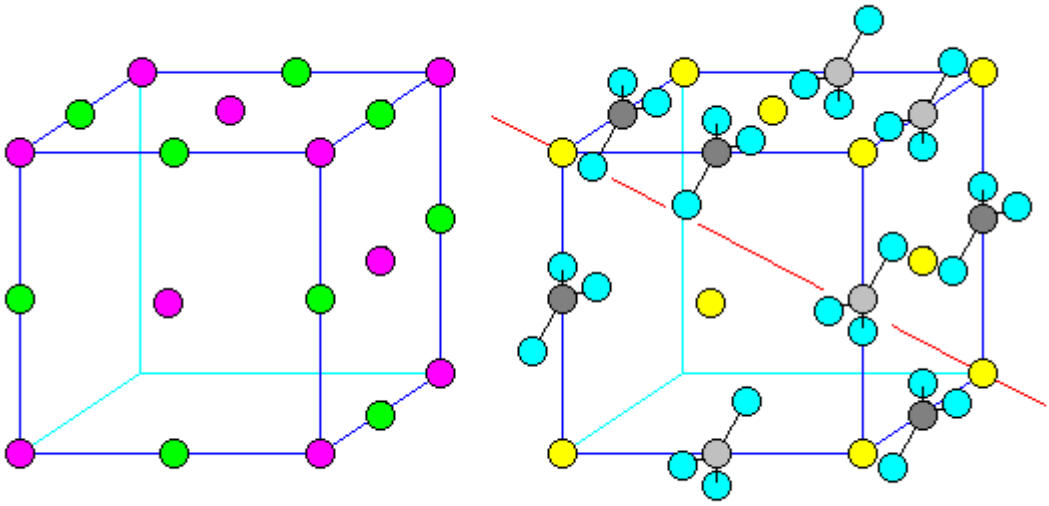

Figure 3.2 The likeness between NaCl and $CaCO_3$

The structure of calcite is not very complex but can be hard to visualize. It is sometimes described as a "modified NaCl" structure.

On the left in (Fig.3.2) is the structure of NaCl, with sodium atoms purple and chlorine atoms green (although since both have the same atomic arrangement, it hardly matters). On the right in (Fig.3.2) is calcite, with calcium yellow, oxygen blue and carbon gray. We can see that there are rows of alternating Ca and CO_3 units, just like Na and Cl alternate in halide.

Calcite is not cubic. The carbonate groups break up the cubic symmetry in several ways. First, their three-fold symmetry axes line up with only one of the symmetry axes of the cube (in red). Second, they alternate in orientation (shown by the two shades of gray) (Fig.3.2). Calcite has got trigonal crystal system. Calcite can be in various colors. Varieties of calcite is anthraconite, stain spar, iceland spar, prasochrome, aphrite, argenite e.g. Mn, Fe, Zn, Co, Ba, Sr, Pb e.g. are found

common impurities in calcite. Calcite can be dangerous in view of health. There is no specific data on health dangers or toxicity for this mineral, however you should always treat mineral samples as potentially toxic dangerous and use sensible precautious when handling them [20 -21].

3.2.2. Defect within the Crystal Structure

The alkali halides structure consists of an orderly arrangement of alkali and Halide ions, one after another, alternating in all three directions. Figure (3.3) shows the structure of two ideal crystals.

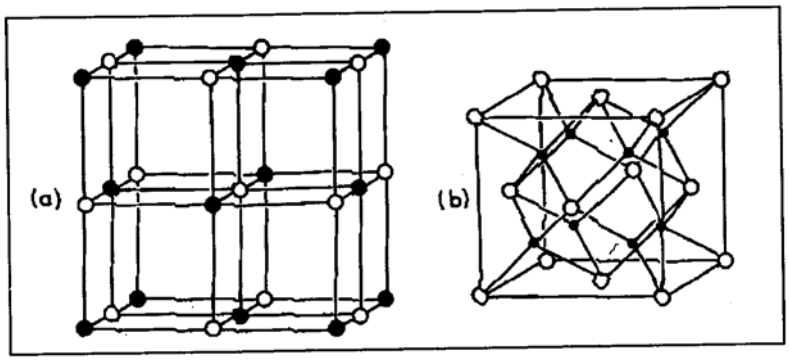

Figure 3.3 The three-dimensional structure of an ideal crystal:
(a) Structure of LiF (• Li, o F); (b) structure of CaF_2 (• Ca, o F).

At the contrary, a real crystal possesses defects which are basically of three general types: (Fig. 3.4 depicts three types defects)

1. First types defect is the intrinsic or native defects, they can be:

a) vacancies or missing atoms (called schottky defects): A vacancy is a defect obtained when one atom is extracted from it's site and not replaced.

b) interstitial or frenkel defect: It consists of an atom an atom x inserted in a crystal x in a non-proper lattice site.

c) substitutional defects: for example, halide ions in alkali sites.

d) aggregate forms of previous defects

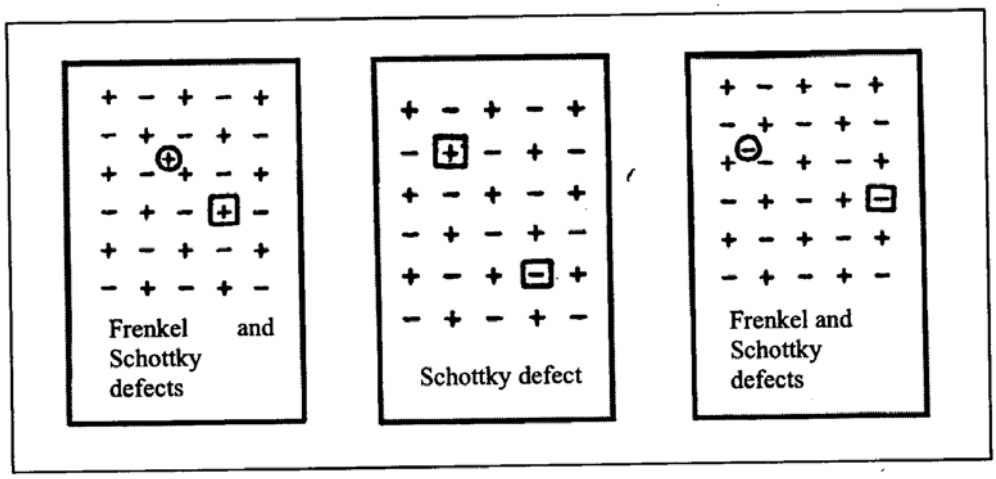

Figure 3.4 Structures of a real crystal with intrinsic defects: i.e. LiF, + alkali ion (Li^{+}), - halide ion (F^{-}), [+] alkali ion vacancy, [-] halide ion vacancy, ⊕ interstitial alkali ion, Θ interstitial halide ion.

2. Second types defect is extrinsic or impurity defects, like chemical impurities Y in a crystal X, they can be:

a) substitutional impurity: an atom Y takes the place of an atom X.

b) interstitial impurity: an atom Y is inserted in an additional site not belonging to the perfect crystal.

As an example, Fig.3.5 shows the behavior of the divalent cation Mg^{+2} in LiF: it substitutes a Li ion.

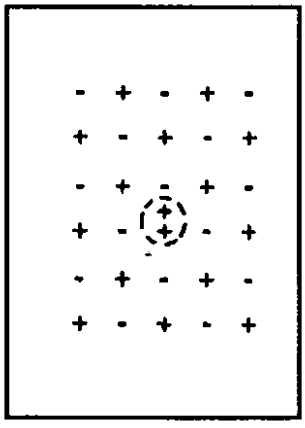

Figure 3.5 Substitutional divalent cation impurity Mg^{2+} in an alkali halides crystal.

To understand the mechanism of chemical impurities, one can see the influence of a divalent ion on vacancy concentration, as shown in Fig.3.6 (a): in order to compensate for the excess positive charge of impurity, an alkali ion must be omitted; furthermore, since the divalent cation impurity is a local positive charge and the cation vacancy is a local negative charge, the two attract each other giving rise to a complex as shown in Fig.3.6 (b).

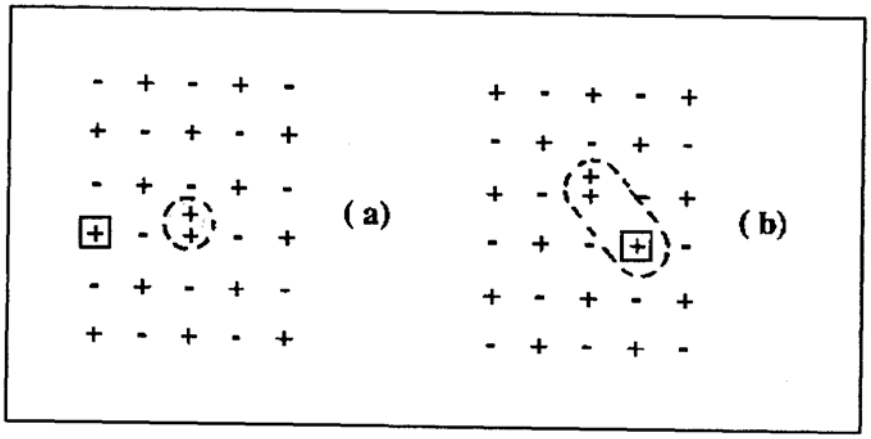

Figure 3.6 (a) an alkali ion missing; (b) attraction of ions to form a complex.

3. Third types defect is ionizing radiation produces further defects in alkali halides.

These defects are called color centers which are absorption centers, coloring ionic crystals. For example, negative ion vacancies are regions of localized positive charge, because the negative ion which normally occupies the site is missing and the negative charges of the surrounding ions are not neutralized. As a result of ionizing radiation, an electron is free to wonder in the crystal and it can be attracted by a Coulomb force to the localized positive charge and can be trapped in the vacancy. This system or centre is called F center (Fig. 3.7).

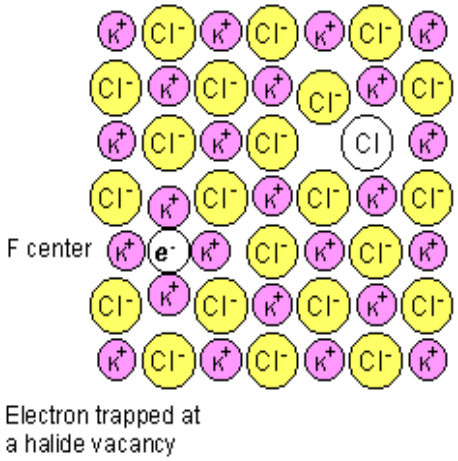

Figure 3.7 F center in alkali halide crystal.

Similarly, a positive ion vacancy represents a hole trap and the system is called V center. Other types of hole centres are possible:

- the V_k centre is obtained when a hole is trapped by a pair of negative ions,
- the V_3 centre which consists of a neutral halogen molecule which occupies the site of a halogen ion: in effect two halide ions with two holes trapped.

The V, V_k ,V_3 defects are shown in Fig.3.8.

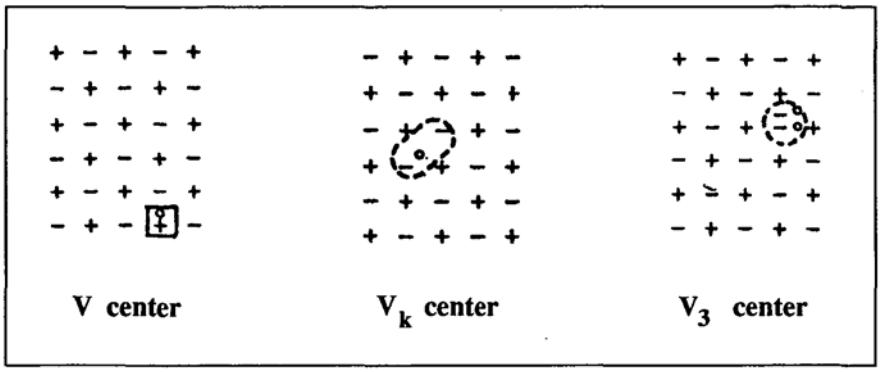

Figure 3.8 V, V_k and V_3 centers in a real crystal.

We have to outline the importance of the defect production during irradiation because high dose levels can induce unwanted effects in TL materials, generally

called radiation damage, which are important in the set up and maintenance of a thermoluminescent dosimetric system, i.e., lowering in sensitivity, saturation effects and so on.

For this reason a phenomenological short feature of radiation damage in crystals is given below.

Photons, electrons, neutrons, charged and uncharged particles can create defects by displacement in the sense that the bombarding radiation displaces the crystal atoms from their normal position in the lattice, producing vacancies and interstitials. The number of defects produced is proportional to the flux of irradiation and to the irradiation time. However, during a long irradiation the number of defects produced will gradually decrease because the possibility of vacancy-interstitial recombination increases.

These impurities either add into the crystal structure from the melt, or diffuse or implant at a later stage [16].

3.3. Theoretical Background of Thermoluminescence

Thermoluminescence consists of a perturbation of the electronic system of insulating or semiconducting materials. Thermoluminescence is a temperature-stimulated light emission from a crystal, after removal of excitation (i.e. ionizing radiation); thermoluminescence is a case of phosphorescence observed under condition of steadily increasing temperature is called glow-curve. A glow-curve may have one or more maxima, called glow-peaks, each corresponding to an energy level trap [22, 23].

3.3.1. Energy Bands, Electronic Transitions in Crystalline Materials and Recombination Process

An insulator like an alkali crystal can be described quantum mechanically by the band model. The conduction band is separated from the valance band by the forbidden region. The solution of the Schrödinger equation for electrons subjected to a periodically varying potential reveals that the allowed energies for the electrons lie only in “allowed zones”.

Thermoluminescence requires the perturbation of a system from a state of thermodynamic equilibrium, via the absorption of external energy, into a metastable state. This is then followed by a thermally stimulated relaxation of the system back to its equilibrium condition.

Figure 3.9 shows an energy diagram for a crystal having a certain number of defects distributed between the conduction band (CB) and the valence band (VB). In thermal equilibrium condition, i.e. T = 0K, all the defect levels, up to the Fermi level F, are occupied by electrons. The electrons and crystal lattice are in thermal equilibrium.

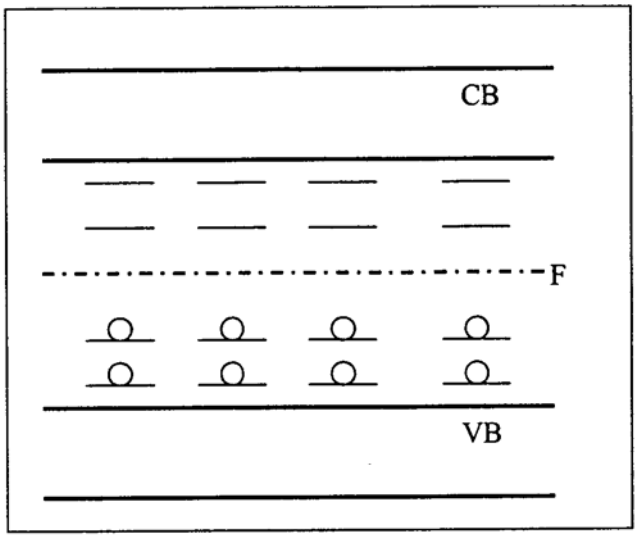

Figure 3.9 a. Energy diagram for a crystal having a certain number of defects distributed between the CB and the valence band VB. The open circles are the electrons.

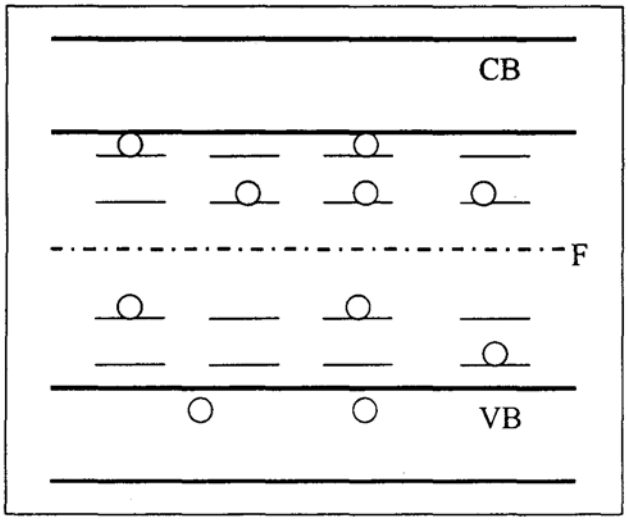

Figure 3.9 b. Redistribution of the trapped electrons due to the irradiation.

The occupancy of each zone, or band, is described by the density of states function, namely N (E) = Z (E). f (E) where f(E) is the Fermi – Dirac distribution function given by f (E) = **Error!**. In these equations, N (E) is the density of occupied energy states, Z (E) is the density of available energy state, and Ef is the Fermi level or, chemical potential [17]. The energy level of highest occupied orbital in a metal at absolute zero is called the Fermi level. Some metals, the Fermi level lies at or near the center of the band. At temperature 0^0K, electrons thermally populate above the Fermi level, and some energy levels just below it remain unoccupied. In this case of a metal, the thermal populations of different energy states cannot be described in terms of a Boltzmann distribution, but are instead given by the Fermi-Dirac distribution [24]. The energy levels introduced may be discrete, or may be distributed depending upon the exact nature of the defect and of the host lattice. In general terms, it is believed that the lattice imperfections, impurities, intrinsic and extrinsic defect give rise to the localized energy levels (metastable state) within the forbidden gap.

The system can now be perturbed by an ionizing radiation. Under irradiation the electrons in the defect levels or in the valence band gain energy and rise into higher levels, beyond the Fermi level (Fig3.9.a). After the irradiation a redistribution process takes place and the excited system goes back to equilibrium (Fig3.9.b). The time required for going back to equilibrium may vary from milliseconds to years, depending on the material, its defects and the temperature [16].

All thermoluminescence phenomena are governed by process of electron-hole recombination. Three distinct types of recombination transition are possible, namely band – to – band, band – to – centre and centre – to – centre The band – to – band recombination may be termed ‘direct’ whilst recombination involving localized levels, i.e., the counters, may be termed ‘indirect’ [17]. (Fig. 3.10)

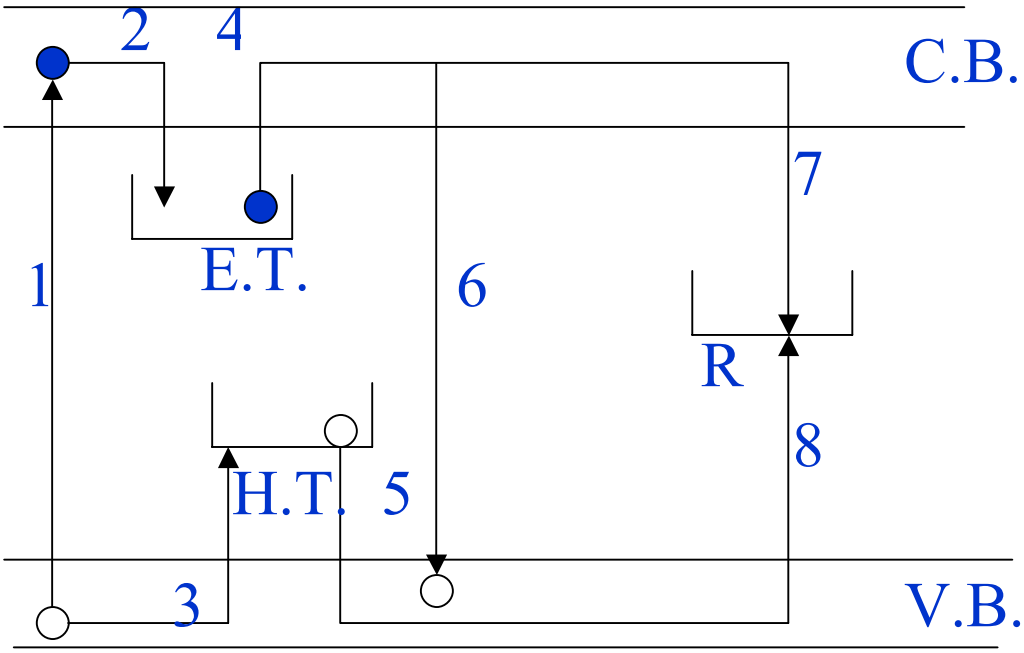

Figure 3.10 Common electronic transitions in semiconductor or insulator: (1) ionization; (2) electron trapping; (3) hole trapping; (4) and (5) electron and hole release; (6) direct recombination; (7) and (8) indirect recombination.

During absorption of light in the far ultraviolet or irradiations with α, β and γ correspond to the liberation of an electron from the valance band into the conduction band leaving a hole in the valance band (transition (1)). Thus, transition (1) corresponds to the process of ionization. The free electron in the conduction band and free hole in the valance band wander through the crystal until they become trapped at the lattice defects. The electron may be trapped by a transition to the lowest available energy level at the defect (transition (2)). The hole may be also be trapped at a lattice defect above the valance band (transition (3)). The trapped electrons and holes may be released from the traps when the crystal is heated or under the optical excitation (transition (4) and (5)). When the charge carriers are released to their corresponding band, they are once again free to move trough the crystal and may recombine with a charge carrier of opposite sign, either directly (transition (6)), or indirectly (transition (7) and (8)) [25].

It should be noted that there are two types of luminescent centre. The first are defects which accept a charge and then are complete, so they cease to act as luminescent centres. The second are recombination centers at which electrons and holes annihilate. The latter may be small in number but can act as luminescence centers so long as both electrons and holes are free. Such centers are also important in photoconductivity measurements.

3.4. Models for Thermoluminescence

3.4.1. Simple Model

The free electrons and holes are created in pairs and are annihilated in pairs, there must exist an equal population of trapped holes at level R. The simplest model for TL consists of a single type of electron defect level and a single type of electron defect level in the forbidden gap. In a simple TL model two level are assumed, one situated below the bottom of the conduction band and the other situated above the top of the valance band (Fig. 3.11).

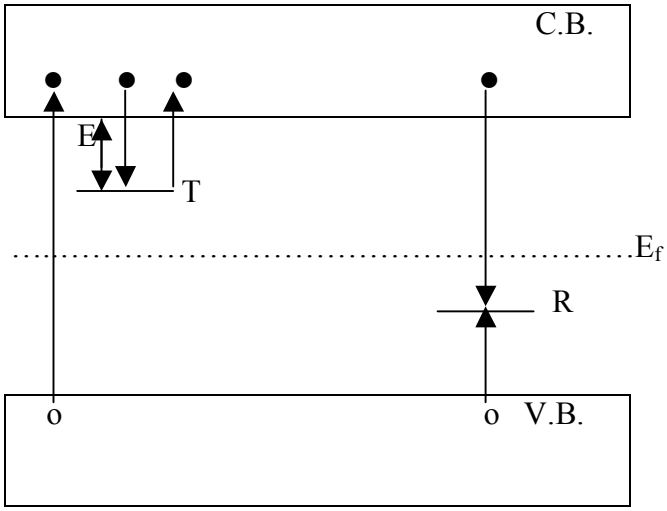

Figure 3.11 Energy band model showing the electronic transitions in a TL material according to a simple two-level model.

The intensity of the thermoluminescence I (t) at any time during the heating is proportional to the rate of recombination of holes and electrons at level R. If n_h is the concentration of trapped holes [17]

$$I(t) = - dn_h/dt \qquad (3.1)$$

As the temperature rises the electrons are released and recombination takes place reducing the concentration of trapped holes and increasing the thermoluminescence intensity. As the electron traps are progressively emptied the rate of recombination decreases and thus the thermoluminescence intensity decreases accordingly. The thermoluminescence is displayed as a function of time. Usually, in an experiment of this type, the temperature is raised as a linear function of time according to

$$T = T_0 + \beta t \qquad (3.2)$$

Where β is defined as the heating rate given by **Error!**= β

The charge carrier being thermally released from it's trap is exponentially related to -**Error!** where E is the trap and the edge of the corresponding delocalized band. The distinction between a trap and a recombination centre, based on the relative probabilities of trapping and recombination, leads to the possibility that, at a given temperature, there will exist a defect level for which these transition probabilities are equal. Such a level, of depth D, would represent a demarcation between the traps and the recombination centre, such that a centre of energy depth E, where E<D, would be a trap, whereas if E>D, the site would be recombination centre. Because the 'depth' of the trap refers to the energy difference between the localized level and the associated delocalized band (i.e., conduction band for electrons; valance band for holes), we have demarcation level for electrons, D_c, and corresponding one for holes, D_h. The demarcation levels are shown in Figure 3.12. Then the range of temperature over which the thermoluminescence peak appears is related to the trap depth .In fact the position of the maximum in a thermoluminescence experiment is determined by the combination of E and s. For given s, one would expect that the larger the values of E (i.e. ,the deeper, the trap) the higher the temperature T_m at which the peak occurs. In this way a thermoluminescence experiment may, under favourable circumstance, provide pertinent information on the distribution of trapping states in a phosphor.

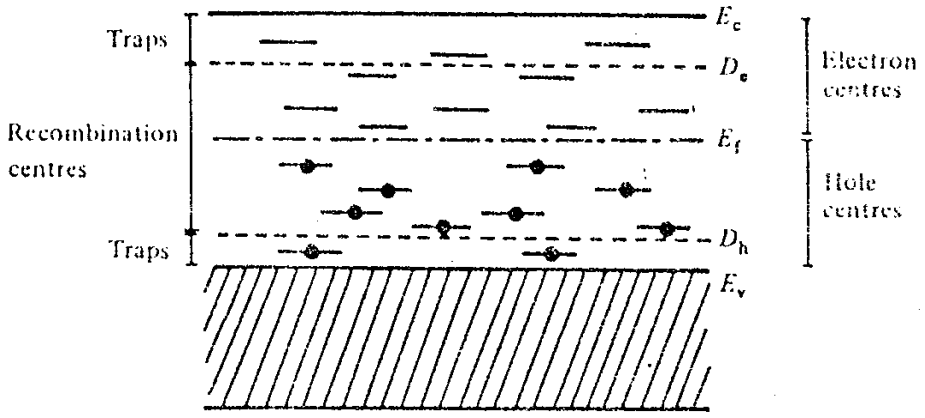

Figure 3.12 Energy level in an insulator in equilibrium at absolute zero. The levels below E_f are full of electrons, while those above are empty.

The probability of charge carrier being thermally released from it's trap is exponentially related to Arrhenius equation, which gives the mean time, τ, that an electron spends in a trap at a given temperature T [26]. It is

$$\tau = s^{-1} \exp (\textbf{Error!}) \qquad (3.3)$$

where s is the frequency factor (in the case of thermoluminescence the frequency factor (in the case of thermoluminescence the frequency factor is also called attempt-to-escape frequency), E is the energy difference between the bottom of CB and the trap position in the band gap, also called trap depth or activation energy, k is the Boltzmann's constant.

Equation can be rewritten as

$$P = \tau^{-1}$$

$$P = s \, . \exp (- \textbf{Error!}) \qquad (3.4)$$

which gives the probability P, per unit of time of the release of an electron from the trap.

According to equation (3.2), if the trap depth is such that at the temperature of irradiation, let us say T_i, E is much larger than kT_i, electrons produced by irradiation

and then trapped will remain in the trap for long period of time, even after the removal of the irradiation. The Arrhenius equation introduces the concept of an activation energy, E, seen as an energy barrier which must be overcome in order to reach equilibrium.

3.4.2. Trap Filling Process

Following Chen, McKeever-Durrain (1981) the trap filling process may be described by the following four equations [17]:

$$dn_c/d_t = f - n_c A_r n_h - n_c(N-n)A, \quad (3.5)$$

$$dn/dt = n_c(N-n)A, \quad (3.6)$$

$$dn_v/dt = f - n_v(N_h - n_h)A_h , \quad (3.7)$$

$$dn_h/dt = n_v (N_h - n_h)A_h - n_c n_h A_r , \quad (3.8)$$

The terms involved are: n_c – concentration of electrons in the conduction band (per unit volume); n_v – concentration of holes in the valance band; n – concentration of electrons in traps; N – concentration of available electron traps (of depth E below the conduction band); n_h – concentration of holes in recombination centres; N_h – concentration of available hole centres; A transition coefficient for electrons in the conduction band becoming trapped (volume/ unit time); A_h – transition coefficient for holes in the valance band becoming trapped in the hole centers; A_r – recombination transition coefficient for electrons in the conduction band with holes in centers and f – the electron-hole generation rate(volume/unit time).

The transition coefficients to the capture cross-sections by equations of the form $A=\upsilon\sigma$ where υ is the thermal velocity of free carriers in conduction or valence bands and σ is the cross-sections for the capture of the free charges by the trapped charges. Additionally, for charge neutrality it can be seen that;

$$n_c + n = n_v + n_h . \quad (3.9)$$

3.4.3.Trap Emptying Process

Assuming a single electron trap and single hole center, the rate equations describing the flow of charge between various energy levels and bands during trap emptying have been described by Adirovitch (1956) [27], Hearing and Adams (1960) [28], and Halperin and Braner (1960) [29] as

$$dn_c/dt = nsexp(-E/kT) - n_c(N-n)A - n_c n_h A_r \quad (3.10)$$

$$dn/dt = n_c(N-n)A - nsexp(-E/kT) \quad (3.11)$$

$$I_{TL} = -dn_h/dt = n_c n_h A_r \quad (3.12)$$

where I_{TL} is TL intensity (photon/sec).

According to Eqn. 3.11, I_{TL} is equal to the rate of recombinations, which is proportional to the number of recombination centers and the number of free electrons. Unfortunately, there is no general analytical solution of this Eq.3.10, 3.11, 3.12; however, an approximate solution can be achieved by making some assumptions. Alternatively, numerical solutions can be found for a given set of the parameters E, s, A_r, A, N, N_o, n_o, n and n_h [30-31]. These numerical solutions are quite useful for studying the dependence of the TL curve on various parameters.

In order to obtain an analytical solution of Eqn. 3.10-3.12, the following two assumptions may be used

$$n_c << n , \qquad dn_c/dt << dn/dt \quad (3.13)$$

It was also assumed that the charge neutrality condition becomes

$$n_c + n = n_h \quad (3.14)$$

which for $n_c \approx 0$ means $n = n_h$ and $dn/dt \approx dn_h/dt$. Since $dn_c/dt \approx 0$, one gets from Eqn. 3.10-3.12;

$$I = -\frac{dn_h}{dt} = \frac{ns\exp\left(-\frac{E}{kT}\right)}{1+\frac{(N-n)A}{nA_r}} \tag{3.15}$$

3.5. Thermoluminescence of Kinetic Analysis

3.5.1. First-order kinetic

I(t) (in Eq.3.15) cannot be solved analytically without additional simplifying assumptions. Randall and Wilkins [32-33] assumed negligible retrapping during the heating stage, i.e. they assumed mA»(N-n)Ar. Under assumption can be written

$$I(t) = -\frac{dn}{dt} = sn\exp\left\{-\frac{E}{kT}\right\} \tag{3.16}$$

This differential equation describes the charge transport in the lattice as a first-order process and the glow peaks calculated from this equation are called first-order glow peaks. Solving the differential equation (3.16) as a function of time yields

$$I(t) = -\frac{dn}{dt} = n_o s\exp\left\{-\frac{E}{kT}\right\}\exp\left\{-s\int_0^t \exp\left\{-\frac{E}{kT(t')}\right\}dt'\right\} \tag{3.17}$$

where n_o is the total number of trapped electrons at time t=0.Usually the temperature is raised as a linear function of time according to

$$T(t) = T_0 + \beta t \tag{3.18}$$

with β the constant heating rate and T_0 the temperature at t=0. This gives for the intensity as function of temperature

$$I(t) = -\frac{1}{\beta}\frac{dn}{dt} = n_o \frac{s}{\beta}\exp\left\{-\frac{E}{kT}\right\}\exp\left\{-\frac{s}{\beta}\int_{T_0}^{T}\exp\left\{-\frac{E}{kT'}\right\}dT'\right\} \qquad (3.19)$$

This is the well-known Randall—Wilkins first-order expression of a single glow peak. The peak has a characteristic asymmetric shape being wider on the low temperature side than on the high temperature side. On the low temperature side, i.e. in the initial rise of the glow peak, the intensity is dominated by the first exponential (exp(-E/kT)). Thus, if I is plotted as function of 1/T, a straight line is expected in the initial rise temperature range, with the slope of -E/k, from which the activation energy E is readily found.

The properties of the Randall-Wilkins equation are illustrated in Fig.3.13. In Fig.3.13(a) it is shown how 1(T) varies if n_o varies from n_0=0.25 m^{-3} till n_0=2 m^{-3} while E=1 eV, s=1.0x10^{12} s^{-1} and β=1 K/s are kept constant. It can be noted that the temperature at the peak maximum, T_m, stays fixed. This is a characteristic of all first-order TL curves. The condition for the maximum can be found by setting dI/dt=0 (or, somewhat easier from dlnI(T)/dt=0). From this condition one gets

$$\frac{\beta E}{kT_m^{\,2}} = s\exp\left\{-\frac{E}{kT_m}\right\} \qquad (3.20)$$

In this equation n_0 does not appear which shows that T_m does not depend on n_0. From Fig.3.13(a) it can be further seen that not only the peak height at the maximum but each point of the curve is proportional to n_0. In the application in dosimetry n_0 is the parameter of paramount importance since this parameter is proportional to the absorbed dose. It is simple to see that the area under the glow peak is equal to n_0 since

$$\int_0^{\infty} I(t)dt = -\int_0^{\infty}\frac{dn}{dt}dt = -\int_{n_0}^{n_\infty} dn = n_0 - n_\infty \qquad (3.21)$$

and n_∞ is zero for $t \rightarrow \infty$. In Fig.3.13(b) the activation energy E has been varied from 0.8 to 1.2 eV. As *E* increases the peak shifts to higher temperatures with a decrease in the height and an increase in the width keeping the area (i.e. n_0) constant.

Similar changes can be noticed as s is varied (see Fig.3.13(c)) but now in the opposite way: as *s* increases the peak shifts to lower temperatures with an increase of the height and a decrease in width. In Fig.3.13(d) the heating rate has been varied. As β increases the peak shifts to higher temperatures while the height decreases and the width increases just as in the case of decreasing s. This can be expected since s and β appear as a ratio s/β in Eqn.(3.19). It is worthwhile to note that of the four parameters the activation energy *E* and the frequency factor *s* are the main physical parameters. They are called the trapping parameters and are fixed by the properties of the trapping centre. The other two parameters can be chosen by the experimenter by choosing a certain dose (n_o) and by read-out of the signal at a certain heating rate β. lnvestigation of a new TL material will therefore start with studying the glow peak behaviour under variation of the absorbed dose and the heating rate.

The evaluation of Eqn.(3.19) is hampered by the fact that the integral on the right-hand side is not elementary in the case of linear heating. Chen [34] has shown how the integral can be approximated by asymptotic series. In practical applications it is convenient to describe the glow peak in terms of parameters which are easy to derive experimentally, namely the intensity of peak at the maximum I_m and the temperature at the maximum T_m. Kitis et al. [35] have shown that Eqn.(3.19) can be quite accurately approximated by

$$I(T) = I_m \exp\left[1 + \frac{E}{kT}\frac{T - T_m}{T_m} - \frac{T^2}{T_m^{\,2}}\exp\left\{\frac{E}{kT}\frac{T - T_m}{T_m}\right\}(1-\Delta) - \Delta_m\right] \qquad (3.22)$$

with $\Delta = 2kT/E$ and $\Delta = 2kT_m/E$.

Recently Pagonis et al.[36] have shown that a Weibull distribution, which is one of the most commonly used distribution in reliability engineering because of the many shapes it attains for various values of b (slopes) [37], function also accurately describes the first-order TL curve. These expression expressions may be convenient for peak fitting purposes.

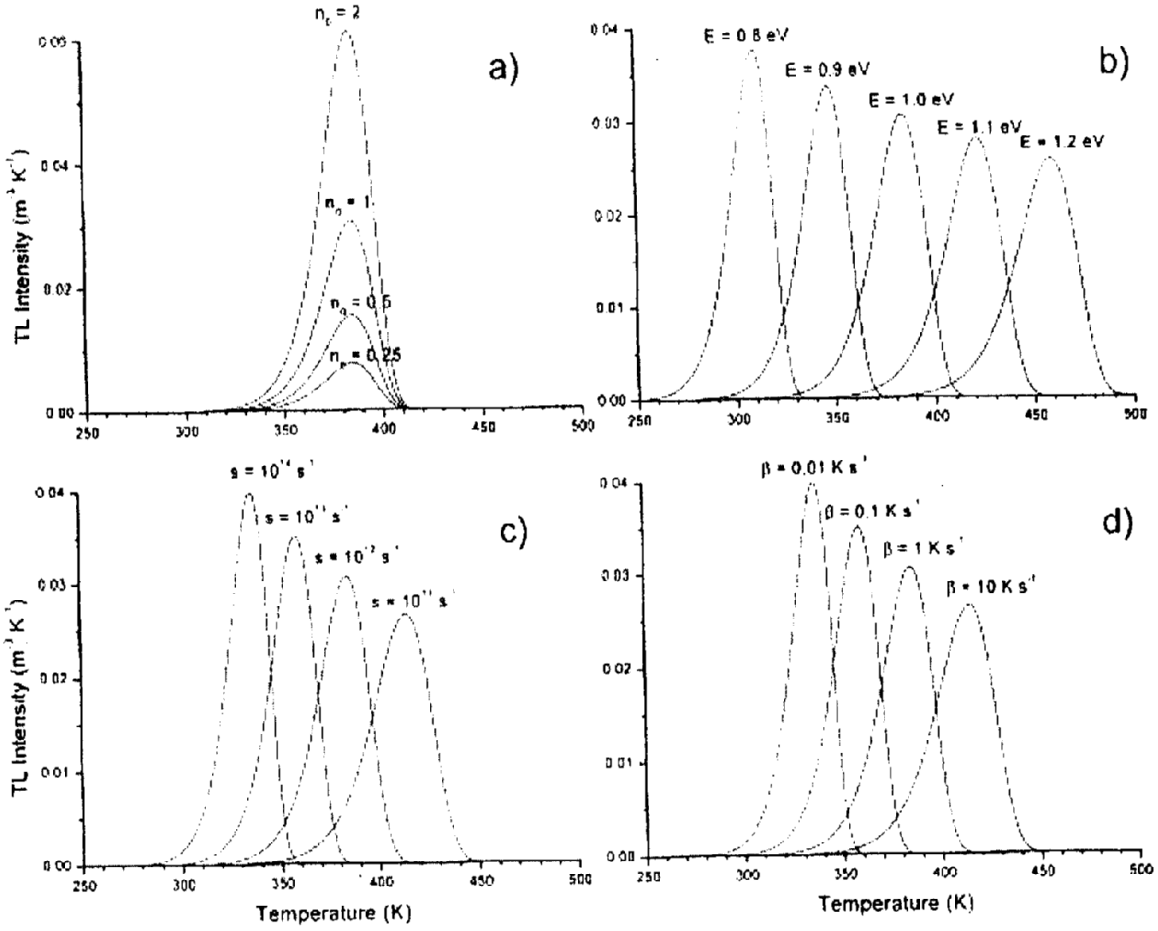

Figure 3.13 Properties of the Randall and Wilkins first-order TL equation, showing: (a) variation with n_0, the concentration of trapped charge carriers after irradiation; (b) the variation with E, the activation energy; (c) the variation with s, the escape frequency; (d) the variation with β, the heating rate. Parameter values: n_0=1 m^{-3} E=1 eV; s=lx 10^{12} s^{-1}, β=1 K/s of which one parameter is varied whi1e the others are kept constant.

3.5.2. Second-order kinetics

Garlick and Gibson [38] considered the possibility that retrapping dominates, i.e. mA«(N-n)A_r. Further they assume that the trap is far from saturation, i.e. N»n and n=m. With these assumptions, Eqn.(3.15) becomes

$$I(t) = -\frac{dn}{dt} = s\frac{A}{NA_r}n^2 \exp\left\{-\frac{E}{kT}\right\} \tag{3.23}$$

We see that now dn/dt is proportional to n^2 which means a second-order reaction. With the additional assumption of equal probabilities of recombination and retrapping, $A=A_r$, integration of Eqn.(3.23) gives

$$I(T) = \frac{n_0^{\,2}}{N}\frac{s}{\beta}\exp\left\{-\frac{E}{kT}\right\}\left|1+\frac{n_0 s}{N\beta}\int_{T_0}^{T}\exp\left\{-\frac{E}{kT'}\right\}dT'\right|^{-2} \tag{3.24}$$

This is the Garlick—Gibson TL equation for second-order kinetics. The main feature of this curve is that it is nearly symmetric, with the high temperature half of the curve slightly broader than the low temperature half. This can be understood from the consideration of the fact that in a second-order reaction significant concentrations of released electrons are retrapped before they recombine, in this way giving rise to a delay in the luminescence emission and spreading out of the emission over a wider temperature range. The initial concentration n_0 appears here not merely as a multiplicative constant as in the first-order case, so that its variation at different dose levels change the shape of the whole curve. This is illustrated in Fig.3.14(a). It is seen that T_m decreases as n_0 increases. It can be derived [39] that the temperature shift can be approximated by

$$T_1 - T_2 \approx T_1 - T_2\frac{k}{E}\ln f \tag{3.25}$$

where T_1 is the temperature of maximum intensity at a certain dose and T_2 the temperature of maximum intensity at f times higher dose. With the parameter values of Fig.3.14(a) the shift is 25 K. When E=1 eV, T_1=400 K and the absorbed dose is increased by a factor 1000, which is easy to realise experimentally, a temperature shift of 77 K can be expected. From Eqn.(3.25) it follows further that for a given increase of the dose the shallower the trap, i.e., the smaller E, the larger the peak shift. Fig.3.14(b) illustrates the variation in size and position of a second-order peak as function of E, in Fig.3.14(c) s function of s/N, and in Fig.3.14(d) as function of the

heating rate. The area under the curve is, as in the case of first-order kinetics, proportional to the initial concentration n_0 but the peak height is no longer directly proportional to the peak area, although the deviation is small.

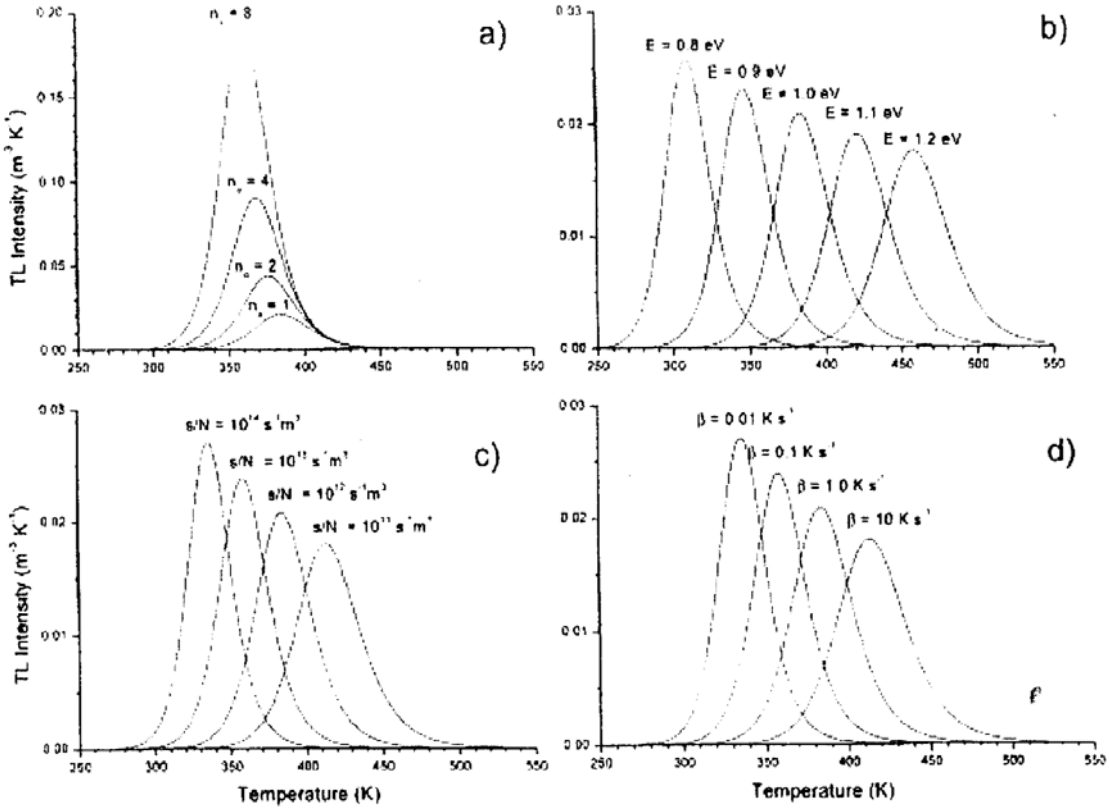

Figure 3.14 Properties of the Garlick—Gibson second-order TL equation, showing: (a) variation with n_0, the concentration of trapped charge carriers after irradiation; (b) the variation with *E*, the activation energy; (c) the variation with s/N; (d) the variation with β, the heating rate. Parameter values: n_0=1 m^{-3}; E=1 eV; s/N=1x10^{12} s^{-1} m^{-3}, β=1 K/s of which one parameter is varied while the others are kept constant.

Note that, similarly to the first-order case, the term dominating the temperature dependence in the initial rise is exp(-E/kT). So the 'initial rise method' for the determination of the trap depth can be applied here as well.

Also for second-order kinetics the glow peak shape, Eqn.(3.24) can be

approximated ‘with a function written in terms of maximum peak intensity I_m and the maximum peak temperature T_m [35]

$$I(T) = 4I_m \exp(\frac{E}{kT}\frac{T-T_m}{T_m}) \times \left[\frac{T^2}{T_m{}^2}(1-\Delta)\exp\left\{ \frac{E}{kT}\frac{T-T_m}{T_m} \right\} + 1 + \Delta_m \right]^{-2} \quad (3.26)$$

with Δ and Δm the same meaning as in Eqn.(3.22).

3.5.3. General-order kinetics

The first- and second-order forms of the TL equation have been derived with the use of specific, simplifying assumptions.

However, when these simplifying assumptions do not hold, the TL peak will fit neither first- nor the second-order kinetics. May and Partridge [40] used for this case an empirical expression for general-order TL kinetics, namely

$$I(t) = -\frac{dn}{dt} = n^b s' \exp\left\{ -\frac{E}{kT} \right\} \quad (3.27)$$

where s’ has the dimension of $m^{3(b-1)}\ s^{-1}$ and b is defined as the general-order parameter and is not necessarily 1 or 2. Integration of Eqn.(2.19) for b≠1 yields

$$\mathrm{I(T)} = \frac{s'}{\beta} n_0 \exp\left\{ -\frac{E}{kT} \right\} \left[1 + (b-1)\frac{s'}{\beta}\int_{T_0}^{T} \exp\left\{ -\frac{E}{kT'} \right\} dT' \right]^{-b/(b-1)} \quad (3.28)$$

where now s”=sn_0^{b-1} with unit s^{-1}. Eqn.(3.28) includes the second-order case (b=2) and reduces to Eqn. (3.19) when b→1. It should be noted that according to Eqn. (3.27) the dimension of s’ should be $m^{3(b-1)}\ s^{-1}$ that means that the dimension changes with the order b which makes it difficult to interpret physically. Still, the general-order case is useful since intermediate cases can be dealt with and it smoothly goes to first- and second-orders when b→1 and b→2, respectively (see Fig.3.15).

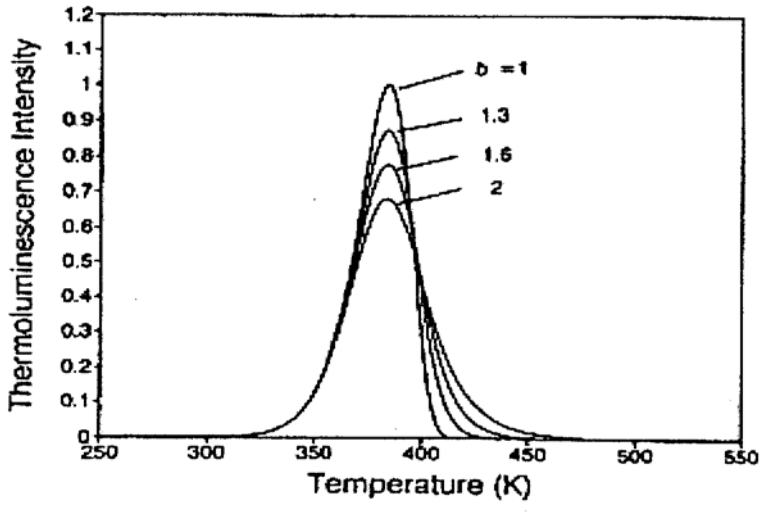

Figure 3.15 Comparison of first-order (b=1), second-order (b=2) and intermediate-order (b=1.3 and 1.6) TL peaks, with E=1 eV, s=1x 10^{12} s^{-1}, n_0=N=1 m^{-3} and β=1 K/s (from [35]).

CHAPTER 4

THERMOLUMINESCENCE ANALYSIS

4.1. Trapping Parameter Determination Method

There are various methods for evaluating the trapping parameters from the glow curves [32-33-41-43-44]. When one glow peak is highly isolated from the others, the experimental methods such as initial rise, variable heating rates, isothermal decay, and peak shape methods are suitable methods to determine these parameters.

In case of overlapping peaks there are essentially two ways to obtain these parameters, the first one is the partial thermal cleaning method and the second one is the computer glow curve deconvolution program. In most cases, the partial thermal cleaning method can not be used to completely isolate the peak of interest without any perturbation on it. Therefore, the computer glow curve deconvolution program become very popular method to evaluate trapping parameters from TL glow curves in recent years [42].

4.2.1. Peak Shape Method

The first peak shape method was developed by Grossweiner [45], later Chen [43] modified Halperin and Braner's equation [46] for calculating *E* values.

Chen [47] derived expression for evaluating E using numerical approximations. The Chen method is useful for a broad range of energies ranging between 0,1 eV and 2.0 eV and pre-exponential factors between 10^5 sec^{-1} and 10^{13} sec^{-1} and it does not make any use of literative procedures. Furthermore, the method does not need any knowledge of the kinetics order which is directly found from the peak slope.

It's method is based on the shape of TL peak, similarly to the Lushchik [48] and Halberin – Braner method [49]. For simplicity, the parameters involve in a well resolved peak are here reported in Fig.4.1

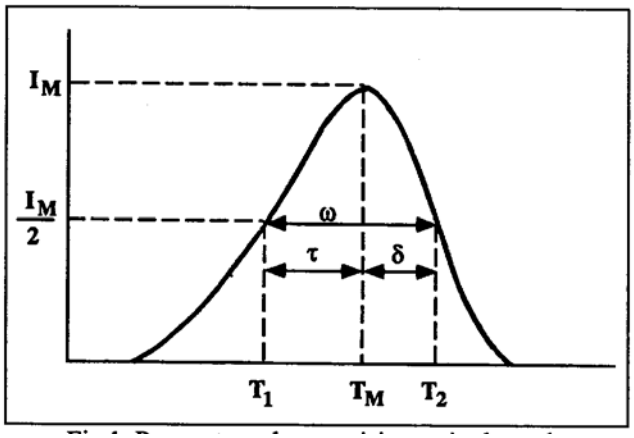

Figure 4.1 Parameters characterizing of single peak.

where T_m, T_1, *and T2*: are respectively the peak temperature at the maximum and the temperatures on either side of the temperature at the maximum, corresponding to half intensity,

$\tau = T_M - T_1$: is the half-width at the low temperature side of the peak,

$\delta = T_2 - T_M$: is the half-width towards the fall-off of the glow peak,

$\omega = T - T_1$: is the total half-width,

$\mu_g = \delta/\omega$ is the symmetrical geometrical factor (shape parameter).

The order of kinetics b can be estimated by means of shape parameters. Chen [44] found that μ_g is not sensitive to changes in E and *s*, but it changer with the order of kinetics b. It has been shown that the ranges of μ_g varies from 0,42 for b=1 to 0,52 for b=2 in case of linear heating.

Interpolating and extrapolating the constants appearing in the equations for the first and second order, Chen gave a general expression which summarizes all the previously given expressions.

$$E_\alpha = c_\alpha \left(\frac{kT_M^{\,2}}{\alpha} \right) + b_\alpha (2kT_M) \qquad (4.1)$$

where α is τ, δ or ω. The values of c_α and b_α are summarized as:

$c_\tau = 1.51+3.0(\mu_g - 0.42)$ $\quad b_\tau=1.58+4.2(\mu_g - 0.42)$

$c_\delta = 0.976+7.3(\mu_g - 0.42)$ $\quad b_\delta=0$ (4.2)

$c_\omega= 2.52+10.2(\mu_g - 0.42)$ $\quad b_\omega=1$

with

μ_g=0.42 for 1st order

μ_g=0.52 for 2nd order

Chen [50] calculated a graph of μ_g, ranging from 0.36 to 0.55 for values of b between 0.7 and 2.5 which can be used for the evaluation of b from a measured μ_g (see Fig.4.2).

Another graph has been proposed by Balarin [51] which gives the kinetics order as a function of $\gamma = \delta/\tau$ (Fig.4.3).

Once the activation energy is obtained, one can find the frequency factor using the following equation

$$s = \left(\frac{\beta}{T_M^{\,2}}\right)\left(\frac{E}{k}\right)\frac{1}{1+(b-1)\left(\frac{2kT_M}{E}\right)}\exp\left(\frac{E}{kT_M}\right) \qquad (4.3)$$

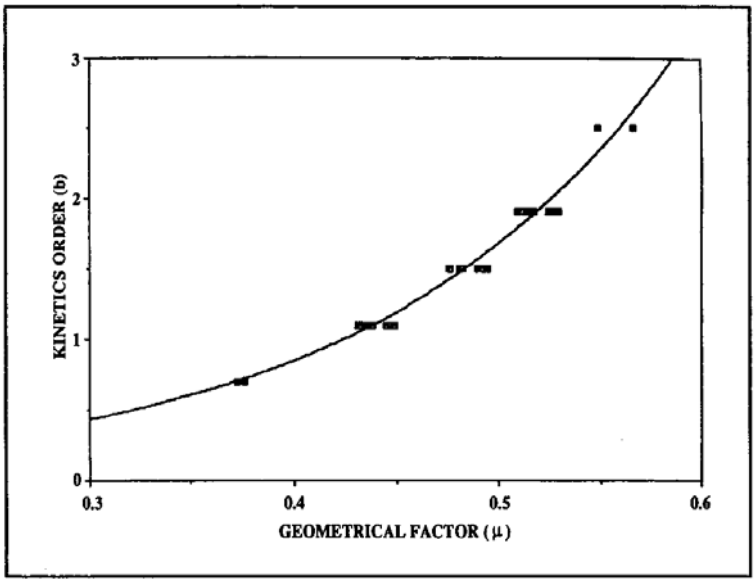

Figure 4.2 Plot of the kinetics order b as a function of the geometrical factor $\mu_g=\delta/\omega$ [52].

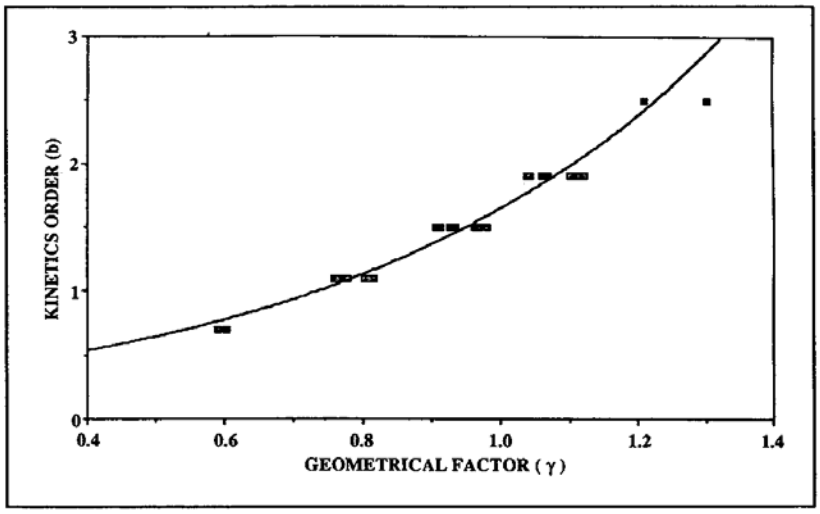

Figure 4.3 Plot of the kinetics order b as a function of the geometrical factor $\gamma=\delta/\tau$ [52].

4.1.2. Isothermal Decay Method

The isothermal decay is quite a different method of analysis of the trapping parameters in which the TL sample temperature is kept constant and the light

emission can be recorded as a function of time. Formerly the isothermal decay method was illustrated for the first-order kinetics by Garlick and Gibson [53]. Generally, in the isothermal decay method, the following equation is solved for constant T for the first order kinetics where n_0 is the initial value of *n* and

$$I(T) = --c\frac{dn}{dt} = c\frac{n_0}{\tau}\exp\left(-\frac{t}{\tau}\right) \tag{4.4}$$

$$\tau = s^{-1}\exp\left(\frac{E}{kT}\right) \tag{4.5}$$

The above equation shows that at a constant temperature T, the light emission will decay exponentially with time t and a plot of ln(I) against t will give a straight line with a slope m = s exp(- **Error!**).

Let the initial integral light be S_0, while S_{ti}. will be the integral light at time t_i:

$$\begin{aligned} S_0 &= n_0 \\ S_{t1} &= n_1 = n_0\exp(-pt_1) \\ S_{tn} &= n_n = n_0\exp(-pt_n) \end{aligned} \tag{4.6}$$

at T=const

Making the ratios

$$\ln\left(\frac{S_{t1}}{S_0}\right) = -pt_1 \ldots\ldots\ldots\ldots \ln\left(\frac{S_{tn}}{S_0}\right) = -pt_n \tag{4.7}$$

the graphs of $\ln(S_{ti}/S_0)$ versus t_i, is then plotted for data obtained at a given storage temperature T. Using different storage temperatures (T_i) one can obtain a set of straight line of slopes

$$m_i = -s\exp\left(-\frac{E}{kT_i}\right) \tag{4.8}$$

from which

$$\ln (m_i) = \ln(-s) - \frac{E}{kT_i} \tag{4.9}$$

Therefore a plot of ln(m) versus 1/T yields a straight line of slope –E/k and intercept ln(-s) on the ordinate axis.

If the experiment is carried out with two different constant storage temperatures, T_1 and T_2, two different slopes, m_1 and m_2, are obtained and then from

$$\ln\left(\frac{m_1}{m_2}\right) = \frac{E}{k}\left(\frac{1}{T_2} - \frac{1}{T_1}\right) \tag{4.10}$$

The last equation allows to calculate E.

$$E = \frac{k}{\left(\frac{1}{T_2} - \frac{1}{T_1}\right)} \ln\left(\frac{m_1}{m_2}\right) \tag{4.11}$$

The frequency factor s substitution of the E value in Eqn. (4.8)

The isothermal decay method is not applicable to higher order kinetics. In 1979; a method has been proposed by Kathuria and Sunta [54] to calculate the order of kinetics from the isothermal decay of thermoluminescence. According to this method; if the decaying intensity from the sample is held at a constant temperature, the plot of $I^{(1/b-1)}$ versus t gives a straight line, when the proper value of b is chosen. Therefore, various b values are tried and the correct one is that giving a straight line.

4.1.3 CGCD Method

Computer Glow Curve Deconvolution (CGCD) is one of the most important method to determine trapping parameters from TL glow curves. This method has the advantage over experimental methods in that they can be used in largely overlapping-peak glow curves without resorting to heat treatment.

The program was developed at the Reactor Institute at Delft, The Netherlands [55]. This program is capable of simultaneously deconvoluting as many as nine glow peaks from glow curve. Two different models were used in the computer program. In the first model, the glow curve is approximated from first order TL kinetic by the expression

$$I(T) = n_0 s \exp\left(-\frac{E}{kT}\right)\exp\left[\left(-\frac{skT^2}{\beta E}\right)*\left(0.9920-1.620\frac{kT}{E_n}\right)\right] \quad (4.12)$$

In the second model the glow curve is approximated with general order TL kinetics by using the expression,

$$I(T)=n_0 s \exp\left(-\frac{E}{kT}\right)\left[1+\left(-\frac{(b-1)s}{\beta}\frac{kT^2}{E}\exp\left(-\frac{E}{kT}\right)*\left(0.9920-1.620\frac{kT}{E_a}\right)\right)\right]^{\frac{b}{b-1}} \quad (4.13)$$

where n_0 (m^{-3}) is the concentration of trapped electrons at t=0, s (s^{-1}) is the frequency factor for first-order and the pre-exponential factor for the general-order, E (eV) the activation energy, T (K) the absolute temperature, k (eVK^{-1}) Boltzmann's constant, β ($°Cs^{-1}$) heating rate and b the kinetic order.

The summation of overall peaks and background contribution can lead to composite glow curve formula as shown below

$$I(T) = \sum_{i0=1}^{n} I(T) + a + b\exp(T) \quad (4.14)$$

where *I(T)* is the fitted total glow curve, a allows for the electronic noise contribution to the planchet and dosimeters infrared contribution to the background.

Starting from the above equation (4.14), the least square minimization procedure and also FOM (Figure of Merit) was used to judge the fitting results as to whether they are good or not. i.e.

$$FOM = \sum_{i=1}^{n}\frac{|N_i(T)-I(T)|}{A} = \sum_{i=1}^{n}\frac{|\Delta N_i|}{A} \quad (4.15)$$

where N_i (T) is the i-th experimental points (total n=200 data points), I(T) is the i-th fitted points, and *A* is the integrated area of the fitted glow curve.

From many experiences [56-57], it can be said that if the values of the FOM are between 0.0% and 2.5% the fit is good, 2.5 % and 3.5% the fit is fair, and> 3.5% it is bad fit.

To have a graphic representation of the agreement between the experimental and fitted glow curves, the computer program also plots the function,

$$X(T) = \frac{N_i(T) - I_i(T)}{\sqrt{I_i(T)}} \tag{4.16}$$

which is a normal variable with an expected value 0 and $\sigma = 1$ where $\sigma^2(T) = I_i(T)$.

4.1.4.Initial Rise Method

The simplest, and most generally applicable method for evaluating the activation energy E of a single TL peak is the initial rise method. The basic premise upon which this method is based that at the low temperature end of the peak, all the relevant occupancies of the states, the trap, and the recombination center and, in some cases, other interactive states can be considered as being approximately constant.

The rise of the measured intensity as a function of temperature in this region is, therefore, very close to exponential, thus

$$I(T) = C \exp\left(-\frac{E}{kT}\right) \tag{4.17}$$

where the constant C includes all the dependencies on the other parameters and occupancies, E is the activation energy (eV), k is the Boltzmann's constant (eV/K^{-1}) and T is the temperature (K).

Plotting In(I) against 1/T a linear plot is obtained with slope equal to -E/k. Hence it is possible to evaluate E without any knowledge of the frequency factor s by means of equation

$$E=-k\frac{d(\ln I)}{d(1/T)} \tag{4.18}$$

Once the value of E was determined, the frequency factor (s) was obtained from the equation

$$\frac{\beta E}{kT_m} = s\exp\left(-\frac{E}{kT_m}\right) \tag{4.19}$$

where T_m, is the temperature at the maximum intensity. This method can only be used when the glow peak is well defined and clearly separated from the other peaks.

4.2.5.Heating Rate Method

Another important method is various heating rates for the determination of activation energies. If a sample is heated at two different linear heating rates β_1 and β_2 the peak temperatures will be different. Equation (4.19) can therefore, be written for each heating rate and dividing the equation for β_1 (and T_{m1}) by the equation for β_2 (and T_{m2}) and rearranging, one gets an explicit equation for the calculation of E

$$E=k\frac{T_{m1}T_{m2}}{T_{m1}-T_{m2}}\ln\left[(\frac{\beta_1}{\beta_2})(\frac{T_{m2}}{T_{m1}})^2\right] \tag{4.20}$$

The major advantage of the heating rate method is that it only requires data to be taken at a peak maximum (T_m, I_m) which, in case of a large peak surrounded by smaller satellites, can be reasonably accurately determined from the glow curve. Furthermore the calculation of E is not affected by problems due to thermal quenching, as with the initial rise method.

When various heating rates for the first-order kinetics are used, the following expression is obtained:

$$\ln(\frac{T_m^{\ 2}}{\beta}) = (\frac{E}{k})(\frac{1}{T_m}) + cons\tan t \qquad (4.21)$$

A plot of ln (T_m/β) versus ($1/ T_m$) should yield a straight line with a slope E/k, then E is found. Additionally, extrapolating to $1/T_m = 0$, a value for ln(sk/E) is obtained from which s can be calculated by inserting the value of E/k found from the slope.

This method of various heating rates are applicable for general-order kinetics which includes the second-order case. For the general order case, one can plot $ln\ [I_m^{b-1} (T_m^2 / \beta)^b\ ]$ versus $1/T_m$, whose slope is equal to E/k.

CHAPTER 5

Experimental Procedure

The materials equipments and experimental procedures utilized in this work are described below.

5.1. Materials

The samples used in this study were calcite crystals obtained from Gaziantep city.

5.2.Equipments

5.2.1. Radiation Source and Irradiation Procedure

The samples were irradiated at room temperature immediately after quenching. Calcite crystals were irradiated with ^{90}Sr-^{90}Y β-source. The activity of β-source is about 100 mCi. It is calibrated by manufacturer on March, 10 1994. The recommended working life-time is about 15 years. Stronium-90 emit high energy beta particles from their daughter products (^{90}Sr-0.546 MeV together with ^{90}Y β-2.27 MeV). Beta radiation is absorbed by air, so its intensity declines with distance much more rapidly than inverse square law calculations would indicate. The maximum range of Y-90 beta particles in air is approximately 9 meter. The irradiation equipment is an additional part of the 9010 Optical Dating System which is purchased from Little More Scientific Engineering, UK [58]. The irradiation source equipment interfaced to PC computer using a serial RS-232 port. Our irradiation source gives 0.015 Gy at per second. Calcite crystals were irradiated to various dose levels between ≈0.9 Gy and ≈864 Gy.

5.2.2. TL Analyzer and TL Measurement

The glow curve measurements for calcite crystals were made using a Harshaw TLD System 3500 Manual TL Reader [59]. It economically provides high reliability. The technical architecture of the system includes both the Reader and a DOS-based IBM –compatible computer connected through a standart RS-232 serials communication port to control the 3500 Reader. The basic block diagram of reader is shown in figure 5.1. All functions are divided between the reader and the specialized TLD. Shell software runs on the PC. All data storage, instrument control , and operator inputs are performed on the PC. Signal acquisition and conditioning are performed in the reader. In this way, each glow curve can be analyzed using a best-fit computer program based on a Marquardt algorithm minimization procedure, associated to first order and general order kinetic expressions. The program resolves the individual peak present in the curve, giving the best values for the different peak parameters. The instrument includes a sample change drawer for inserting and removing the TLD elements. The reader uses contact heating with a closed loop feedback system that produces adjustable linearly ramped temperatures from 1 ^{0}C to 50 ^{0}C per second accurate to within ± 1 ^{0}C to 400 ^{0}C in the standart reader.

The Time Profile (TTP) is user defined in three segments: Preheat, Acquire, and Anneal, each with independent times (Pre-read anneal: adjustable 0 to 1000 sec, Linear ramp: adjustable from 1 ^{0}C to 50 ^{0}C per second, Post-read anneal: 0 to 1000 sec) and temperature (Pre-read anneal: room temperature to 200 ^{0}C, Post-read anneal: up to 400 ^{0}C). The typical time temperature profile is shown in figure 5.2. To improve the accuracy of low-exposure readings and to extend planchet life, the 3500 provides for nitrogen to flow around the blanchet. By eliminating oxygen in the planchet area, the nitrogen flow eliminates the unwanted oxygen-induced TL signal. Nitrogen is also routed through the photo-multiplier tube (PMT) chamber to eliminate moisture caused by condensation. Glow curves were measured using a platinum planchet at a linear heating rate of 1 ^{0}C/s. The time duration between irradiation and necessary TL operation was always kept constant at about 1 min, expect for the storage time experiment. For the variable heating rates were varied from 2 to 5 ^{0}C/s.

Each crystal was read out twice and the second readout is considered to be background of reader plus crystal and was subtracted from the first one and all of the analyses have been carried out after subtraction operations.

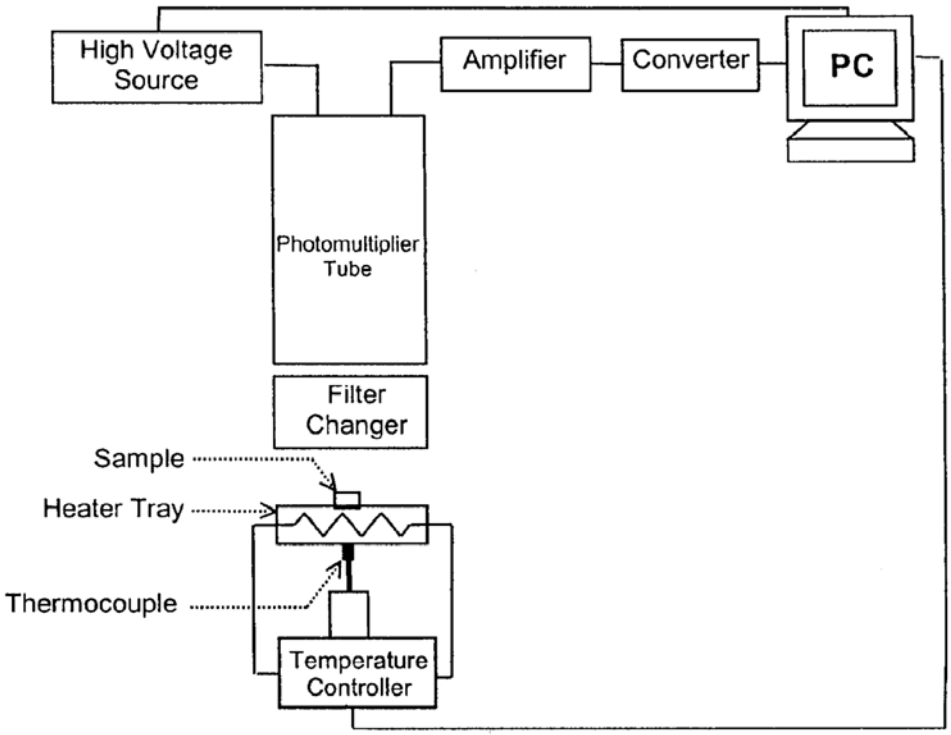

Figure 5.1 Basic block diagram of TL reader

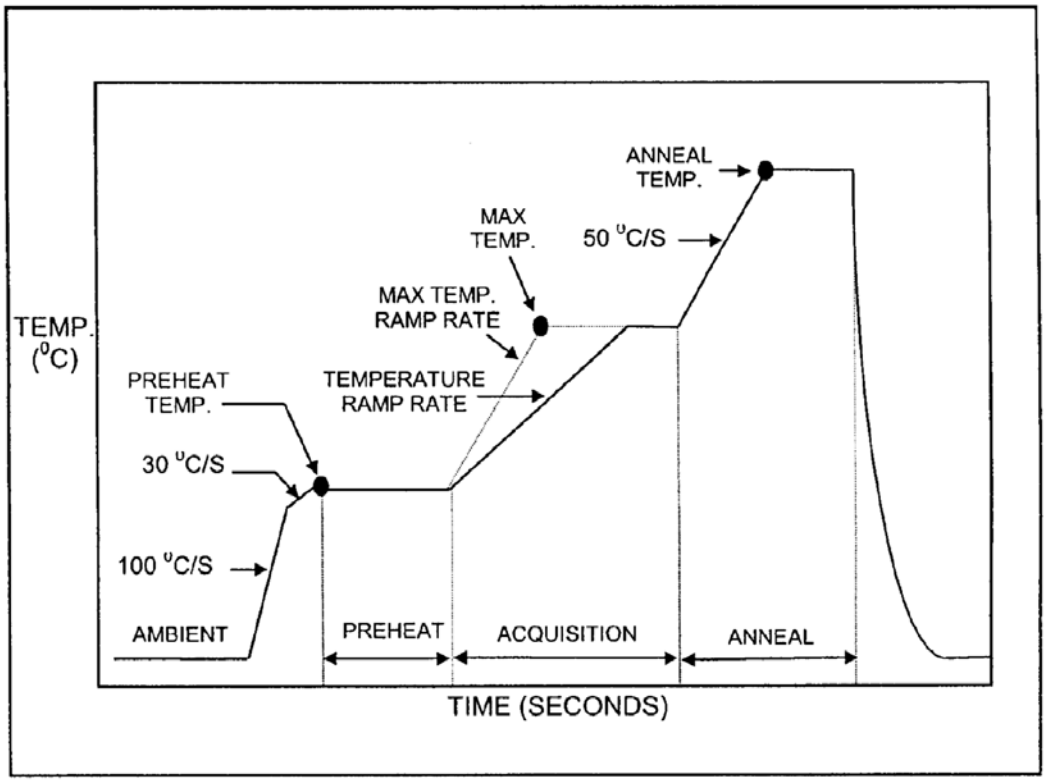

Figure 5.2 Typical time temperature profile (TTP)

5.3. Experimental Procedure for Calcite

The calcite samples, which were in bulk form collected from Gaziantep city, have been taken from geology laboratory in civil engineering of University of Gaziantep.

The samples were heated up to different annealing temperature with different time periods to investigate the suitable annealing temperature and time. The optimum annealing procedure was found to be 500 ^{0}C for 2 hours. The samples was irradiated at room temperature with beta rays from a calibrated ^{90}Sr-^{90}Y source. The irradiated samples were read out in N_2 atmosphere with a Harshaw QS 3500 manual type reader that is interfaced to a PC where TL signals were studied and analyzed. Method that was used to determine kinetic parameters is the variable heating method, VHR. This method is based on the shift position of the temperature at the maximum (T_m) to higher temperatures when the heating rate is increased. For the VHR method, the heating rates were varied from 2 ^{0}C s^{-1} to 5 ^{0}C s^{-1}.

The calcite sample were irradiated at room temperature up to 108 Gy and then they were stored in the dark room at room temperature to evaluate the fading in the intensity of calcite sample.

CHAPTER 6

EXPERIMENTAL RESULTS

6.1. Results and Discussion for Calcite

The determination of E_a and s mainly depends on the prior knowledge of b and exact number of glow curve [60]. We have investigated with two main glow peak in this study. The thermoluminescence (TL) measurements were carried out for the samples annealed in air at the temperature ranging from 50 to 400 ^{0}C. To form an opinion about the b of each individual glow peak, the AD method was firstly used in this thesis. The samples were irradiated at different doses between 0.9 Gy and 864 Gy to check the dose the dependence effect on the peak position. This is the simple test for the first-order kinetics. Some of the selected glow curves after different dose levels are shown in Fig.6.1. In TL theory, the peak temperatures of glow peaks are expected to change only with heating rate for b=1. Hence, for a constant heating rate, the peak maximum should not be affected by other experimental parameters and should thus be fairly constant within the limit of experimental errors. However, for $b\neq1$ and below the trap saturation points {n_0 (concentration of trapped electrons) < N_t (concentration of traps)}, the peak temperatures are shifted to the lower temperature side with increasing dose levels.

As seen from Fig. 6.1, there is no significant change in the position of peak temperatures and they are within the experimental error ±3 ^{0}C for all the doses. This point clearly indicates that the all peaks in the glow curve of calcite should have the first-order kinetics.

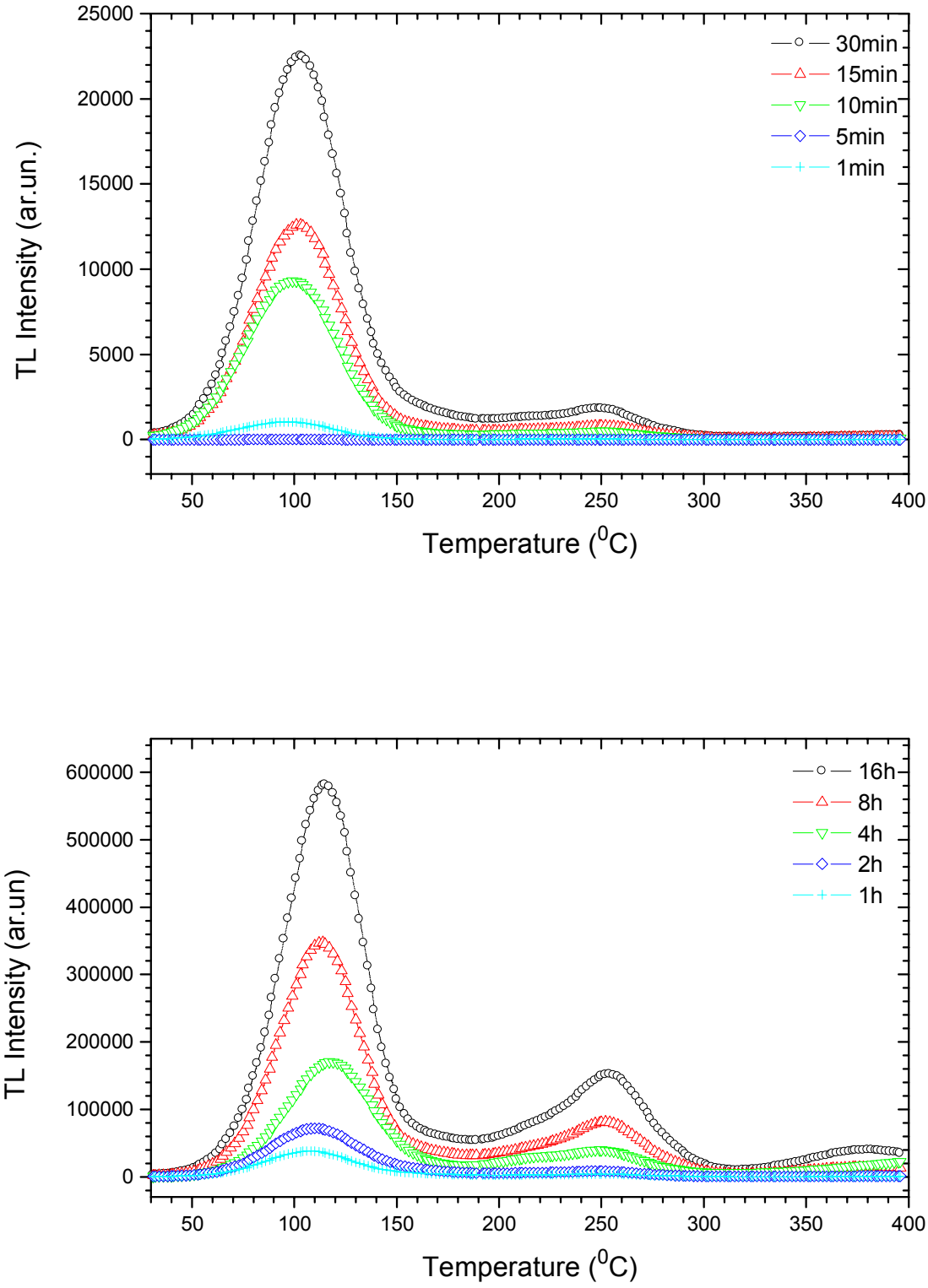

Figure6.1 The glow curves of calcite samples measured after various doses. The sample were firstly annealed at 500 ^{0}C for 2 hours and then irradiated with β-ray at room temperature (β=1^{0}Cs^{-1}).

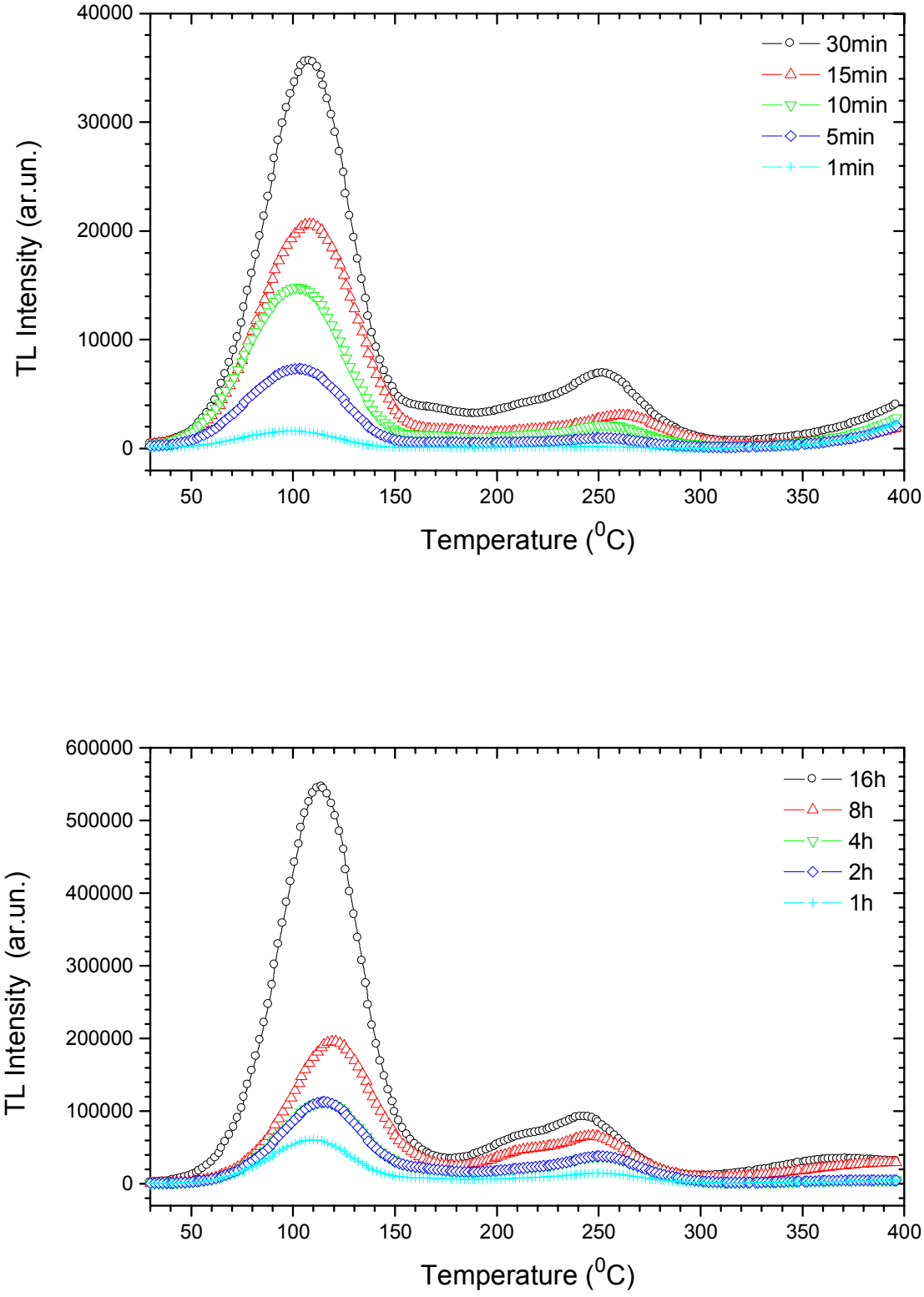

Fig.6.2 The glow curves of calcite samples measured after various doses without the application of heat treatments on the sample ($\beta = 1\ ^0C\ s^{-1}$).

Figures 6.1 and 6.2 show the very marked changes taking place in the shape of TL peak at 115 and 254 ^{0}C when the heat treatments were applied on the samples. Fig. 6.1 and 6.2 show continuous change of the width-at-half maximum of this TL peak as the annealing temperature is changed in the range 50-400 ^{0}C. The glow peaks of width and the kinetic order change as associated in TL process. This effect was previously reported by Medlin (1959) [61]. The annealing may have caused a change in the width of distribution of energy levels E as suggested previously by Medlin (1964) [47]. When the glow curves of annealed and unannealed are compared, it is seen that the intensities of TL peaks of annealed samples are slightly higher than the intensities of TL peaks of unannealed samples. During the partial thermal annealing process, the glow peaks are gradually narrowed with increasing partial thermal annealing temperature and time (Fig.6.1). In addition the glow peak temperature gradually shifted to the high temperature sides with increasing bleaching time and temperature. These behaviour suggest that the glow curve of this sample is the combination of highly overlapped first-order glow peaks or the kinetic orders of all peaks should have higher than first-order kinetics. As the annealing temperature is increased according to the Boltzmann factor exp(-E/kT) until the luminescence center can no longer hold their charges or the trapped charges escape their traps. The ratio of the population in the luminescence center to that of the reservoir trap is low at low annealing temperatures and increases towards unity as the temperature rises. Results of Fig.6.1 and 6.2 show the increase and decrease of height of the TL peak at between 50 and 400 ^{0}C room temperature. The glow curves of annealed sample of intensity are higher than the glow curves of unannealed sample of sensitivity. The intensity of increase was ≈ 10% for 16 hours.

In the given study, the variable heating rate method was firstly applied to obtain the trapping (kinetic) parameters of glow peaks at 115 and 254 ^{0}C. The heating rate were varied between 2 and 5 ^{0}C/sec. (Fig.6.3.). It is known that the major advantage of VHR method is that the required data is to be taken at a peak maximum (I_m, T_m) which, in the case of a large peak surrounded by smaller satellites, can be reasonably accurately determined from the glow curve. But a difficulty arises in the case of highly overlapping peaks with comparable intensities, since the local maximums of some glow peaks in the glow curve are not evident. This problem was overcome by deconvolution of glow curves with computer program. In this respect,

the peak temperatures of peak 1-2 are easily distinguishable from other peak Thereupon, the activation energies of these peaks were calculated by VHR method after determination, of their peak temperatures by choosing their local maximums from glow curves.

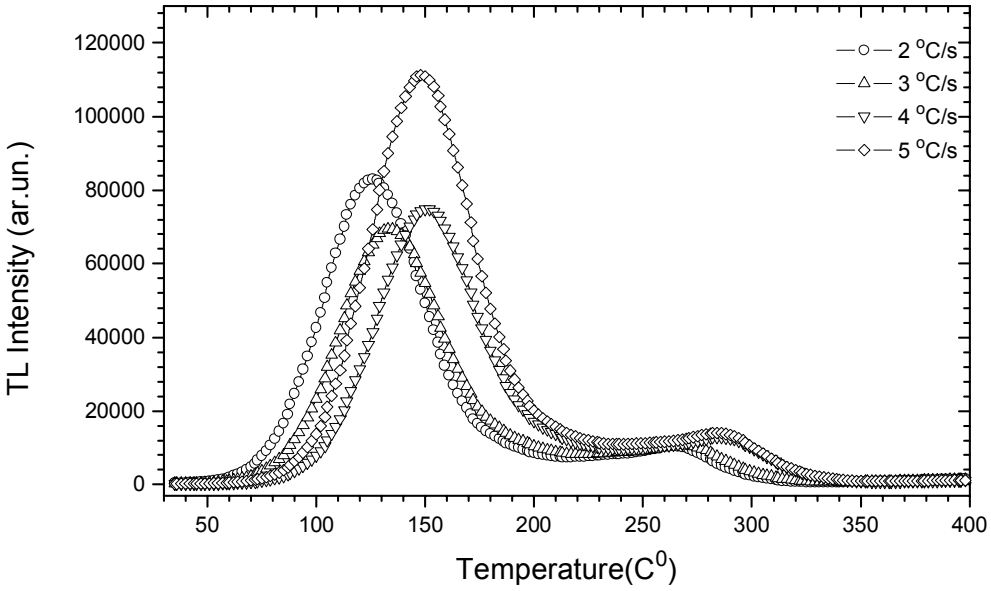

Figure 6.3 The glow curve of calcite sample measured at various heating rates from 2 ^{o}C s $^{-1}$ to 5 ^{o}C s^{-1} after irradiation of samples to a dose level 108 Gy.

Another important point that has to be taken into consideration to avoid large errors in the kinetics parameters determined by VHR method is the temperature lag (TLA) between the heating element and the thermoluminescent sample during the TL readout in readers using contact heating. To avoid this problem, a simple method recently has been proposed by Kitis and Tuyn [62] to correct the TLA and to determine the exact peak temperatures after different heating rates by using the following equations;

$$T_m^j = T_m^i - C\ln(\beta_i / \beta_j)$$

where T_m^j and Tm^i are the maximum temperatures of glow peak with heating rates β_j and β_i, respectively and C is a constant, which is initially evaluated by using two

very low heating rates where the TLA can be considered as negligible. In preference, the low heating rates should be chosen below 1 ^{0}C /s to calculate the constant C. On the other hand, the used TLD reader in the present work does not give permission to low heating rates below 1 ^{0}C /s, there , two intermediate heating rates 1 and 2 ^{0}C/s were used to calculate the constant C and then correct peak maximum positions corrected for the TLA and experimental points. As seen from the figure 6.4., there are slight differences between the slopes, each one giving a different trap depth. From the slope and the graph of the intercept, it was calculated that the energy of peak 1 is E = 0.53±0.1 eV and the frequency factor (s) is ln(s) = 4.737±2.3 sec^{-1}. The calculated kinetic parameters from the slopes and intercepts are given in Table 6.1.

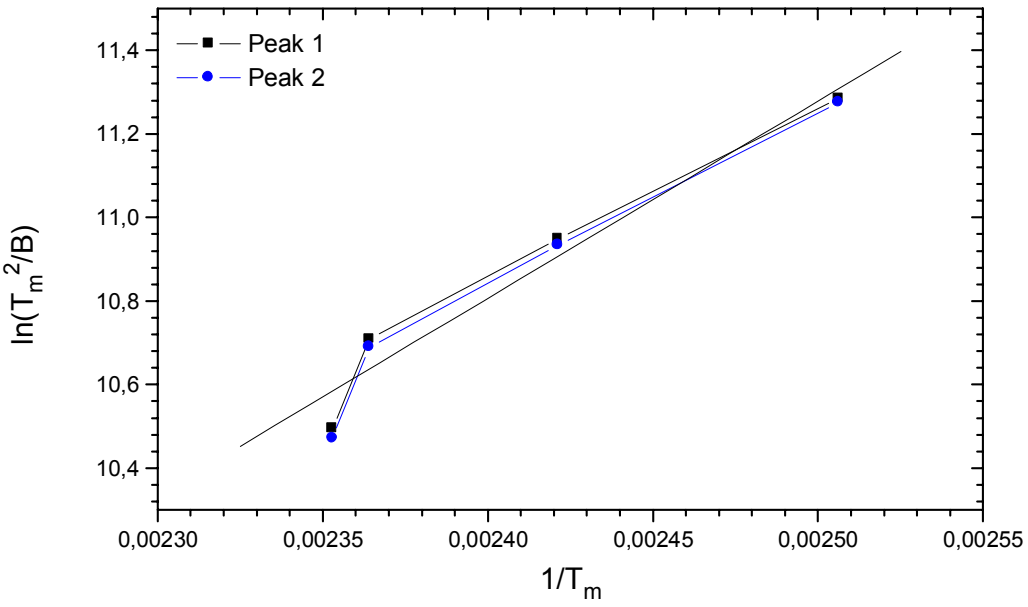

Figure 6.4 Variable heating rate plots of ln(T_m^2/β) against $1/T_m$.

Table 6.1 The values of the activation energy E_a (eV) and frequency factor s (s^{-1}) of TL peaks of calcite determined by the VHR, IR, and PS methods.

Peak No	**$T_m(^0C)(\beta=1\ ^0C/s)$**	**VHR Method**		**IR Method**		**PS Method**		CGCD Method	
		E(eV)	*ln(s) s^{-1}*	*E(eV)*	*ln(s)s^{-1}*	*E(eV)*	*ln(s)s^{-1}*	*E (eV)*	*ln(s)s^{-1}*
1	115	0.531±10	4.737±2.3	0.830±0.01	27.88±0.36	0.546±0.003	12.98±0.002	*0.8* ±0.01	*0.211.10*²±0.3
2	254	0.930±0.2	1.68±2.4	-	-	-	-		

The stability of the stored signal at normal temperatures is an important factor in many applications such as archeological and geological dating, personal and environmental dosimetry, etc. Any appreciable decay in the stored signal at room temperature will invalidate the relationship between TL emitted and the radiations exposure that may have been delivered at some considerable time before readout. The extent of TL signal decay over long periods is difficult if not impossible to measure directly, particularly in archeological applications. The measured glow curves of calcite at the end of the planned storage periods are shown in figure 6.5. As seen from this figure 6.5., the intensity of low temperature peaks 1 is quickly increased while high temperature peaks 2 is not sufficiently influenced from storage periods at room temperature.

After the storage at room temperature for 4 weeks, peak 1 was completely disappeared from the glow curves, but peak 2 did not change during this period. After the storage at room temperature for 2 hours, peak 1 was reduced to typically 36% of its original value and peak 1 reduced to 70% its original value after 6.5 hours at storage during this period.

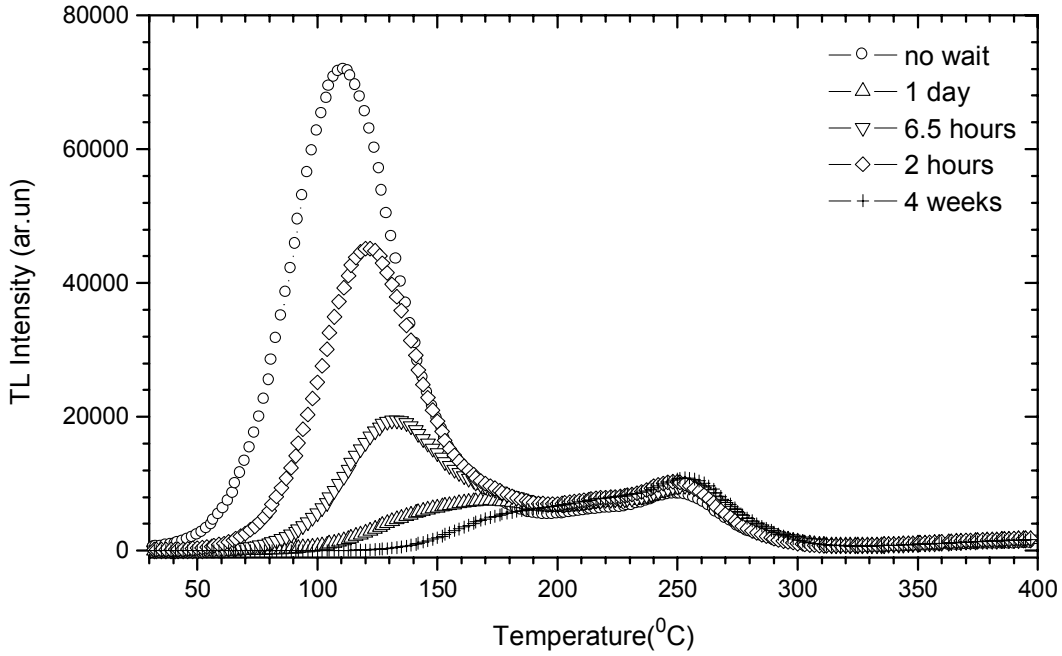

Figure 6.5 Some of the selected glow curves of calcite sample recorded after planned storage periods at room temperatures in the dark room.

The dose response was also investigated by the peak height method for all components in the glow curve of calcite. All data in dose response are plotted on a log-log scale and shown in Fig.6.6. It is clearly seen that the dose response of all components follow similar pattern and strongly linear with slopes of 3, as readily seen in Fig.6.6.

Besides, the slopes of linearity decreases with increasing temperature that means peak 1 has higher dose response than peaks 2 and so on (Fig.6.6). As seen also from Fig.6.6. the sensitivity of annealed samples is much stronger than that of the unannealed samples and therefore minimum detectable dose levels are reduced below 1 Gy with annealing of samples at high temperatures for sufficient period. There is a number of ways to explain the increase in the sensitivity following annealing. One of them might be removal of unknown non-radiative recombination centers and the other might be the creation of additional luminescent centers [63].

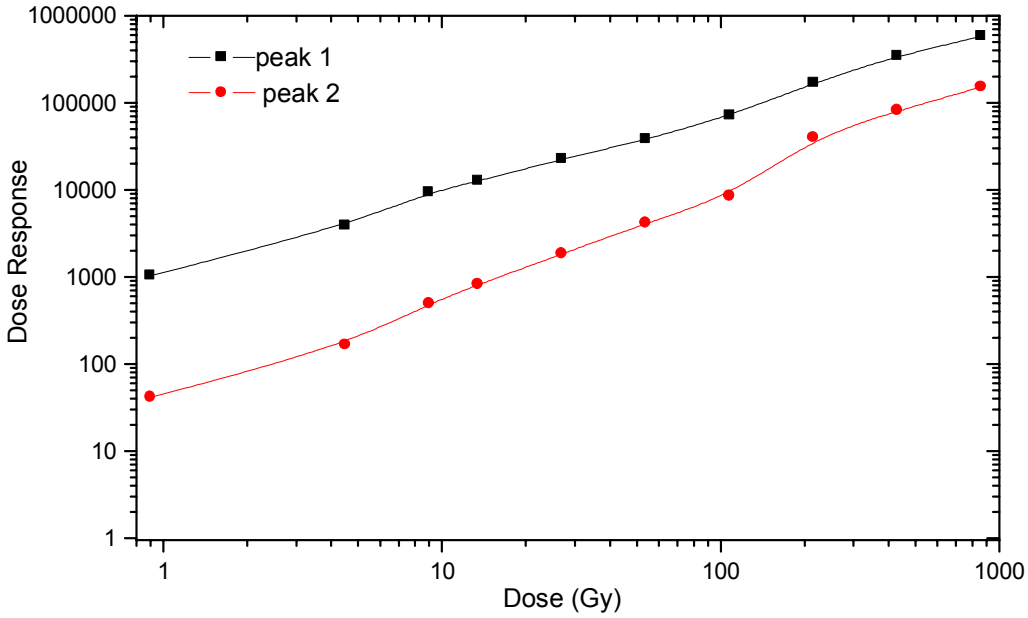

Fig.6.6 The dose response of peaks (P1-P2) determined by peak height method.

We know that in the IR method, plot of *ln(I)* versus $1/T$ would yield a straight line with slope of $-E/k$ and a y intercept of $ln(s/\beta)$, from which E and *s* can readily be calculated. Initial rise method can be used only in the initial region of the TL signal up to ~10% of its peak maximum (I_m). However, if the intensity at the beginning of each peak is very low and especially when the glow curve is composed of several glow peaks, the obtained values of E_a may not reflected the actual values. The average activation energies of our sample are calculated to be 0.830 ± 0.01 eV for P1 (115 ^{0}C) (in the table 6.1.). We have mention that another method that was used to determine the kinetic parameter in the our work is the peak shape method (PS). According to this methods the symmetry factors are calculated for the peak 1 and 2 and found to be $\mu_1 = 0.44$ and $\mu_2 = 0.43$, respectively. These values agree with the first order kinetics (b=1). The activation energies that were calculated by this method were given in table 6.1.

In the analysis of the complex glow curves by CGCD method, it is very important to decide correctly how many glow peaks there are in the glow curve and which of them have first or general-kinetics to obtain results. Especially, the advantages of the CGCD method may be undermined in complex TL glow curves. One may get a local minimum of the least square function which may yield erroneous kinetic attempts to define the best 'best-fit' to the numerical data. As a result, many possible sets of kinetic parameters could be assigned to the same glow curve. The used CGCD program, which is based on the least square minimization procedure, was developed at the Reactor Institute at Delft, The detail results of these models were given in an IRI-CIMAT Report [64]. In the present study, first-order kinetics were approximated for all CGCD evaluations by the expression, Eq.4.12. This method has become very popular method to obtain kinetic parameters. The goodness of fit for all the measured glow curves was tested using the figure of merit (FOM) [65]. From many experience, it can be said that, if the values of FOM are between 0.0% and 2.5% the fit is good, 2.5% and 3.5% is fair fit, and >3.5% is bad fit. In this study, when the evolution of peaks 1and 2 was carefully followed by CGCD method, third peak clearly was observed at approximately 380 ^{0}C when calcite samples were irradiated high doses and calcite sample showed totally big and little 5 peaks during this study, as seen from Fig.6.7. Furthermore; CGCD method is very popular method to evaluate the absorbed dose. The area under the curve is, as in the case of first-order kinetics, proportional to the initial concentration n_0 , the application in dosimetry n_0 is the parameter of paramount importance since this parameter is proportional to the absorbed dose, $n_0 = 0.289.10^8$ and Table 6.1. shows E and s.

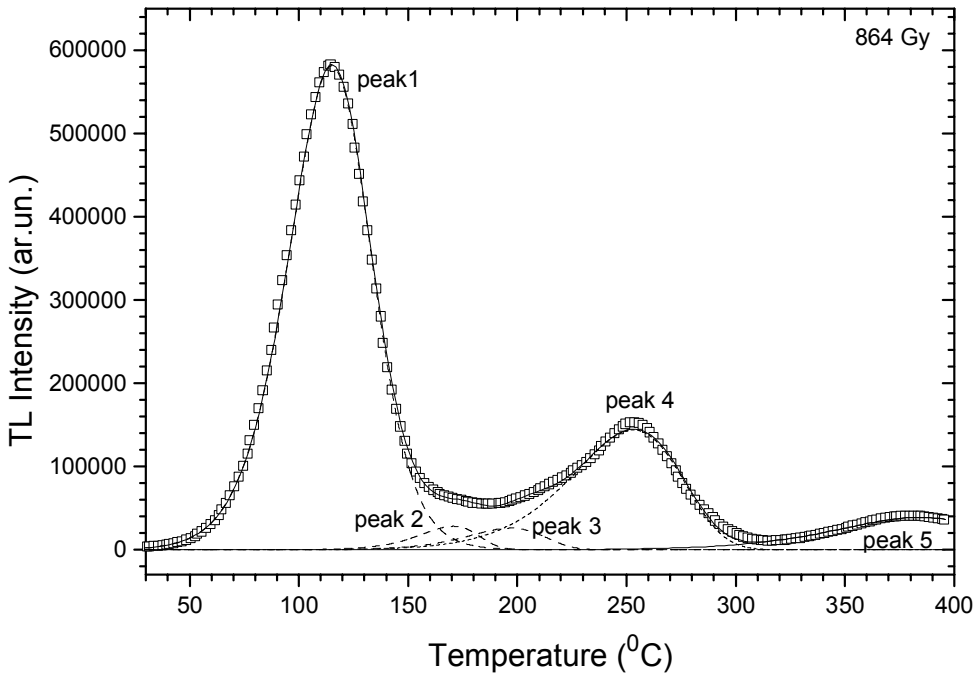

Figure 6.7 The CGCD analyzed glow curves of calcite sample for 864 Gy (FOM = 0.21 %). The open squares represent the experimental points, full curve is the global fitting and broken curves represent fitted individual glow peaks.

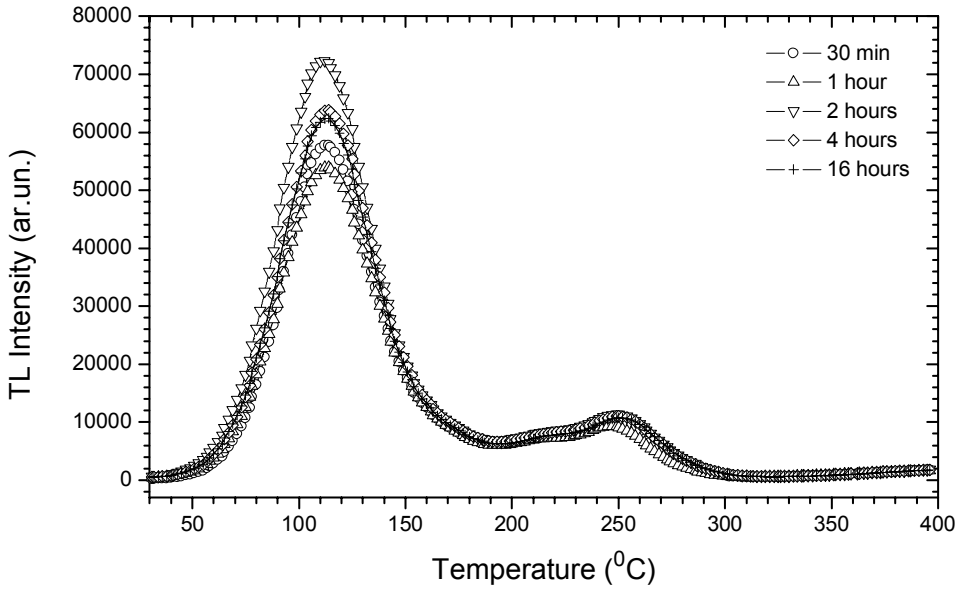

Figure 6.8 The glow curves of calcite sample annealed at 450 ^{o}C with different annealing times.

The enhancement in TL sensitivity was also examined to depend on the annealing temperature and time. The annealing treatment at 500 ^{0}C for 2 hours followed by quenching in air is the optimum conditions for TL sensitization. However; as seen (Fig.6.1.) TL intensity is 590000 ar. un. at 500^{0}C for 16 hours and as seen (Fig. 6.8.) TL intensity is 73000 ar.un. at 450^{0}C for 16 hours. Therefore, the suitable annealing temperature was found to be 500^{0}C.

CHAPTER 7

CONCLUSION

In the present work the glow curves of calcite sample after β irradiation between 0.9 Gy and 864 Gy at room temperature were investigated and two main peaks were studied at 115 ^{0}C and 254 ^{0}C. In addition; third peak was observed at approximately 380 ^{0}C when calcite samples were irradiated at high doses. Additive dose experiments and also peak shape (PS) methods indicate that they are first order kinetics. The activation energies E were found by peak shape (PS) initial rise (IR), computer glow curve deconvolution (CGCD) and variable heating rate (VHR).

The PS method and the VHR method give value of E have shown approximately the same energy value for peak 1. The activation energy of peak 2 was calculated only by VHR method. Furthermore; the IR and CGCD method give approximately the same energy value for peak 1.The IR and CGCD method gives the value E 37 % higher than the value obtained by VHR and PS methods. This study has been supported with analyzing the measured glow curves by CGCD program. When the evaluation of peaks 1and 2 was carefully followed by CGCD method, third peak clearly was observed at approximately 380 ^{0}C when calcite samples were irradiated at high doses and calcite sample showed totally big and little 5 peaks during this study. CGCD method is very popular method evaluate the absorbed dose and trapping parameters of glow peaks from the glow curves. Because, during the curve fitting procedure whole curve is utilized in the analysis, rather than just a few points on the glow curve. The area under the curve is, as in the case of first-order kinetics, proportional to the initial concentration n_0 , the application in dosimetry n_0 is the parameter of paramount importance since this parameter is proportional to the absorbed dose. It is well known that the TL sensitivity of many TL materials depend on the annealing temperature and time. Therefore, the calcite samples which were used in this study were also annealed at different temperatures (400 ^{0}C, 450 ^{0}C and 500^{0}C) for different annealing durations. It was observed that TL sensitivity of

this material is highly dependent on the annealing temperature and time. The suitable annealing temperature was found to be 500 ^{0}C for 2 hours to obtain high intensity. In this case, it was observed that the sensitivity of peak 1 is approximately 10 % higher than the other annealing procedures. Additionally, it was observed that the annealing affects the width of the glow peaks. The full width at half maximum of all peaks decrease with increasing annealing temperature and consequently the annealing affects the evaluated kinetic parameters of main peaks.

The dose responses of all components of annealed and unannealed calcite have similar pattern, first they follow strong linearity and then saturated at different dose levels. When the glow curves of this material stored in the dark room were recorded after 4 weeks, peak 1 was completely disappeared from the glow curves, but peak 2 did not change during this period. After the storage at room temperature for 2 hours, peak 1 it is was reduced to typically 36% of its original value and at the and of 6.5 hours reduced 70% of its original value during this period.

.

REFERECES

[1] P.D. Townsend, J.C. Kelly, Colour Centers and Imperfection in Insulator and Semiconductors, (1973).

[2] C.Furetta, G.Kitis "Review models in thermoluminescence", *Journal of materials science* **39**, 2277, (2004).

[3] McKeever S. W. S, Radiat. Prot. Dosim., **8**, 81 (1984).

[4] Chen R and McKeever S. W. S, Theory of Thermoluminescence and Related Phenomena*, World Scientific*, Singapore, (1997).

[5] M.Urbina, A.Millan, P.Beneitez, T.Calderon."Dose rate effect in calcite", Journal of Luminescence **79**, (1998), 21.

[6] S.Dorendrajit Singh and S. Ingotombi, "Thermoluminescence glow curve of γ-irradiated calcite", J. Phys. D: Appl. Phys., **28**, 1509, (1994).

[7] Y.Kirish, P.D. Townsend and S.Shoval "Local transitions and charge transport in thermoluminescence of calcite", Nucl. Tracks Radiat. Meas. **213**, 115, (1987).

[8] David M, Kathuria S P and Sunta C M, Ind. J. Pure *Appl. Phys*., **20**, 519 (1982).

[9] Horowitz Y. S. and Yossian D., Radiat.Prot.Dosim., **60**, 1 (1995).

[10] Vasilis Pagonish and Chiristodoulos Michaeli, "Annealing effects on the thermoluminescence of synthetic calcite" Elsevier Science **1350**, 131, (1993).

[11] Vasilis Pagonish, Eric Allman and Albert Wooten, "Thermoluminescence from a distribution of trapping levels in UV irradiated calcite, Radiation Measurement **26**, 265, (1985).

[12] B.Engin, O.Güven "The effect of heat treatment on the thermoluminescence of naturally-occurring calcites and their use as a gamma-ray dosimeter", Radiation Measurements **32**, 253, (2000).

[13] Z.S. Macedo, M.E.G. Valerio, J.F. de Lima, "Thermoluminescence mechanism impurity doped calcite", *Journal of Physics and Chemistry of Solids* **60**, 1973,(1999).

[14] J.F. Lima, M.E.G.Valerio and E.Okuno, "Thermally assisted tunneling" P*hysical ReviewB, 64, 014105.* (2001).

[15] V.Ponnusamy, V.Ramasamy, M.Dheenathayalu, J.Hemalatha, "Effect of annealing in thermostimulated luminescence (TSL) on natural blue colour crystals*",.Nucl. Inst. And Methods in Phys. Research,* **217**, 61*,* (2003).

[16] Claudio Furetta, Handbook of Thermoluminescence, (2003).

[17] McKeever S.W.S., Thermoluminescence of Solids, Cambridge University Press (1985).

[18] Chen R. and Kirsh Y., Analysis of thermally Stimulated Processes, *Pergamon Press* (1981).

[19] Zimmermann D.N., *Abstract Symp*. Archaeometry and Archaeological Prospection, Philadelphia (1997).

[20] Jalyon Ralph, Mindat-org mineralogy, (2005).

[21] Steven Dutch, University of Wisconsin, *Natural and Applied Science* (2005).

[22] McKeever S.W.S. and Chen R., "Luminescence Models", *Rad. Measur*. **27** 625, (1997).

[23] Furetta C. and Wengs P.S., "Operational thermoluminescence dosimetry" *World Scientific*, (1998).

[24] Catherine E.H. and A.G.Sharpe, Inorganic Chemistry, (2001).

[25] Yazici A.N., Radiat. Prot. Dosim., *submitted by journal.*

[26] Bube R.H., Photoconductivity of Solids, Wiley and Sons, N.Y. (1960).

[27] Adirovitch E.I *Phys. Rad*, **17**, 705, (1956). ..

[28] Haering R. R. and Adams E.N., *Phys. Rev*., **117**, 451, (1960).

[29] Halperin A. and Braner A.A., 'Evaluation of Thermal Activation Energies from Glow Curves', Phys.Rev., **117**, 405-415, (1960).

[30] Bull K.R., McKeever S.W.S., Chen R., Mathur V.K., Rhodes J.F. and Brown M.D, 'Thermoluminescence kinetics for multipeak glow curves produced by the release of electrons and holes', *J.Phys. D:Appl.Phys*., **19**, 1321, (1986).

[31] Sakurai T 'New method for numerical analysis of thermoluminescence glow curves', *J.Phys. D:Appl.Phys*., **28**, 2139, (1995).

[32] J.T. Randall and M.H.F. *Wilkins Proc.R.Soc.London Ser.* A **184**, 366, (1945).

[33] J.T. Randall and M.H.F. *Wilkins Proc.R.Soc.London Ser.* A **184**, 390, (1945).

[34] R.Chen,in: Y.S. Horowitz (Ed.), Thermoluminescent and Thermoluminescent Dosimetry, Vol. 1, *CRC Press, Boca Raton*, FL, (1984).

[35] G.Kitis, J.M. Gomez-Ros and J.W.N. Tuyn J.Phys.D: *Appl.Phys*. **31**, 2636, (1989).

[36] R.V. Pagonis, S.M. Mian and G.Kitis Radiat. Protect. Dosim. **93**, 11, (2001)

[37] Kececioglu, Dimitri, Reliability Engineering Handbook, Weibull distribution *Prentice Hall*, 1,1991.

[38] G.F.J. Garlick and A.F. Gibson *Proc.Phys.Soc*. **60**, 574, (1948).

[39] A.J.J. Bos and J.B.Dielhof Radiat.Prot.Dosim. **36**, 231, (1991).

[40] C.E. May and J.A. Partridge J.Chem.Phys. **40**, 1401, (1964).

[41] Chen and A.A. Winner J.*Appl.Phys*. **41**, 5227, (1970).

[42] B.Bunghkbardt, D. Singh and E.Piesch, Nuclear Instrument and Methods, **142**, (1977).

[43] Chen R J.*Appl.Physis* **40**, 570, (1969).

[44] Azerin J. Nucl. Tracks **11**, 159, (1986).

[45] Grossweiner L. J. *Appl.Physics* **24**, 1306, (1953).

[46] Halperin A. and Braner A.A. *Phys. Rev*. **117**, 405, (1960).

[47] Medlin W.L., Trapping centers in thermoluminescent calcite. *Phys. Rev.* **75**, A1770-A1779, (1964).

[48] Lushchik C.B., *Phys*. **3**, 408, (1960).

[49] Halperin A. and Braner A.A., *Phys. Rev*. **117,** 408, (1960).

[50] Chen R., J. Electrochem. Soc.*: Solid State Science*, **166**, 1254, (1969).

[51] Balarin M., *Phys. Stat*. Sol., **54**, (1979).

[52] Fruetta C. and Weng P.S. , Operational Thermoluminescence Dosimetry, (1998).

[53] Garlick G.F.J. and Gibson A.F., *Proc. Phys. Soc*. **60,** 574, (1948).

[54] Kathuria S.P. and Sunta C.M. J.Phys.D:*Appl. Phys*. **12**, 1573, (1979).

[55] Bos A.J.J, Piters J.M., Gomez Ros. J.M. and Delgado A. IRI-CIEMAT Report 131-93-005 IRI Delft, (1993).

[56] Mahesk K, Weng P.S. and Furetta C, Thermoluminescence in Solids and its Applications, (1989).

[57] Hsu P.C. and Wang T.K. Radiat. Protect. Dosim., **16**, 253, (1986).

[58] 9010 Optical Dating System User Manual, Dec. 1993.

[59] Model 3500 Manual TLD Reader User's Manual, July 30 1994, Publication No 3500-0-U-0793-005.

[60] Kirsh Y, *Phys. Stat*. Sol. A., **129**, 12, (1992).

[61] Medlin W.L., Thermoluminescence properties of calcite *J.Chem Phys* **30**, 451-458, (1959).

[62] Singth T.S.C., Mazumdar P.S. and Gartia R.K., *Appl.Phys.,***21**, 1312, (1988).

[63] Kristianpoller N, Abu-Rayya M. And Chen R., *Radiat Prot.Dosim*., **33**, 93, (1990).

[64] Bos A J J, Piters J M, Gomez Ros J M and Delgado A, (GLOCANIN, AND Intercomparasion of Glow Curve Analysis Computer Programs IRI CIEMAT Report, 131-93-005IRIDelft.

[65] Misra S K and Eddy N W, *Nucl. Instrum. Meth*. B, **166**, 537, (1979).

.